Title:

Notch mediates inter-tissue communication to promote tumorigenesis.

Authors: Hadi Boukhatmi‡, Torcato Martins, Zoe Pillidge, Tsveta Kamenova and Sarah Bray*.

Address: Department of Physiology Development and Neuroscience, University of Cambridge, Downing Street, Cambridge CB2 3DY, UK

‡ Present address: Centre de Biologie du Développement (CBD), Centre de Biologie Intégrative (CBI), Université de Toulouse, CNRS, UPS, Toulouse, France

* Corresponding author: sjb32@cam.ac.uk

Key words:

Notch, Delta, Zfh1, *Drosophila*, tumor, Inter-tissue signaling, cytonemes,

Summary

Disease progression in many tumor types involves interaction of genetically abnormal cancer cells with normal stromal cells. Neoplastic transformation in a *Drosophila* genetic model of EGFR-driven tumorigenesis similarly relies on the interaction between epithelial and mesenchymal cells, providing a simple system to investigate mechanisms used for the cross-talk. Using the *Drosophila* model, we show that the transformed epithelium hijacks the mesenchymal cells through Notch signaling, which prevents their differentiation and promotes proliferation. A key downstream target in the mesenchyme is Zfh1/ZEB. When *Notch* or *zfh1* are depleted in the mesenchymal cells, tumor growth is compromised. The ligand Delta is highly up-regulated in the epithelial cells where it is found on long cellular processes. By using a live transcription assay in cultured cells and by depleting actin-rich processes in the tumor epithelium, we provide evidence that signaling can be mediated by cytonemes from Delta-expressing cells. We thus propose that high Notch activity in the unmodified mesenchymal cells is driven by ligands produced by the cancerous epithelial. This long range Notch signaling integrates the two tissues to promote tumorigenesis, by co-opting a normal regulatory mechanism that prevents the mesenchymal cells differentiating.

INTRODUCTION

Cells in developing organisms are in continuous communication with their neighbors, with the signals sent and received being crucial for proper organ development. The careful regulation of these signals controls growth, coordination and homeostasis of complex tissues and organs. In contrast, their aberrant regulation or inappropriate deployment is integral to many diseases including cancers. For example, signaling between genetically abnormal cells and the normal surrounding stromal cells supports tumor progression and malignancy, as in many carcinomas [1]. Although mutations driving cancer initiation, such as those causing hyperactivity of the EGFR/Ras signaling pathway, have been extensively characterized [2], it is important also to identify mechanisms that co-opt the surrounding stromal cells to sustain tumor growth. Normal tissue mesenchymal cells are thought to be "educated" within the tumor environment, acquiring properties that in turn enhance cancer cell proliferation and metastasis [3]. A better understanding of the plasticity, regulation and function of tumor mesenchymal cells is therefore important and could influence cancer treatments.

Highly proliferative tumors arise from several genetic manipulations of *Drosophila* wing disc epithelial cells, for example through EGFR pathway hyperactivity in an epigenetically compromised context (*EGFR-psq*^{RNAi}, [4]). These tumors grow as a large multilayer mass, mixing epithelial and mesenchymal cells, providing a simple model to investigate stromal interactions. Although not directly modified, the mesenchymal cells are necessary for tumor growth, since ablating them genetically reduces tumor progression [4]. The mesenchymal cells arise from a pool of myogenic precursors, which normally give rise to tadult flight muscles and to a small number of undifferentiated satellite cells [5, 6]. Maintenance of these precursors under normal conditions requires Notch activity, which directs expression of several genes that help to sustain progenitor characteristics including Zfh1/ZEB [7, 8]. Indeed the ability of the satellite cells to escape differentiation involves upregulation of a short RNA isoform of *zfh1*, *zfh1-short*, that enables the cells to escape regulation by microRNAs [9]. ZEB has a similar function in mammalian precursors [10]. It is unclear however what roles, if any, Notch and/or *zfh1* have in maintaining the tumor mesenchymal cells and in the cross-talk with the cancerous epithelium.

A role for the evolutionarily conserved Notch pathway in regulating the tumor-promoting properties of mesenchymal cells is also suggested by its alterations in cancer-associated

fibroblasts in several tumor types [11, 12]. Whether Notch signaling could also be involved in the inter-tissue communication between the epithelium and mesenchyme has not, however, been explored. Notably, because the ligands are transmembrane proteins, Notch activation relies on direct cell-to-cell contacts. Interactions with the transmembrane, Delta–Serrate-Lag (DSL), family of ligands provokes two cleavages of the Notch receptor to release its intracellular domain (Nicd). This moiety then translocates to the nucleus where it activates the transcription of target genes with its DNA binding-partner CSL [13]. Since the pathway activation relies on cell-to-cell contact, signaling commonly occurs between cells in the same tissue, for example within an epithelium. However, longer range signaling has been found to occur in some circumstances through dynamic cellular process that can extend several cell diameters [14-16]. This raises the possibility that signaling could occur between different tissue types, such as between the tumor epithelium and adjacent stromal/mesenchymal cells.

To determine whether Notch activity in unmodified mesenchymal cells contributes to tumor progression and whether the Notch pathway is involved in cross-talk with the aberrant epithelium, we investigated its role in *EGFR-psq*^{RNAi} tumors [4, 17]. Importantly, this system utilizes an independent LexA targeted manipulation to assess gene functions specifically in the genetically normal mesenchyme, independent from any role in the cancer-driven epithelium [18]. We detect high levels of Notch activity in the tumor-associated mesenchymal cells, where it is required to sustain tumorigenesis, preventing differentiation and promoting proliferation of the mesenchymal cells. Strikingly, the ligand Delta is highly up-regulated in the genetically altered epithelium, but not in the mesenchyme itself, and is present on long cellular processes. Results from live reporting of Notch pathway activation in cell culture and from perturbation of actin rich processes in the Delta-expressing epithelial cells suggest that signaling can occur at long range between the epithelium and neighboring mesenchyme through cell processes. The conserved transcription factor Zfh1/ZEB is an important direct target of signaling in the mesenchymal cells, being required to sustain tumor growth in a similar manner to Notch itself. The contribution of the mesenchymal cells to tumor progression thus relies on Zfh1 and direct Notch activation via cross-talk with the ligand expressing cancerous epithelium.

RESULTS

A large pool of myoblasts, located on the notal part of the wing disc (Figure 1A-B), are maintained as Twist-expressing undifferentiated precursors for a prolonged period, ultimately contributing to adult flight muscles during metamorphosis. Although not directly modified, these precursors, so-called mesenchymal cells, are necessary to sustain the growth of *EGFR-psq*^{RNAi} tumors over many days [4]. These tumors ultimately consist of large multilayer masses, in which epithelial and mesenchymal cells become intermixed (Figure 1C-D**)** [4]. To investigate whether these mesenchymal cells indeed retain progenitor characteristics, we analyzed expression of differentiation genes (e.g. the muscle protein Tropomyosin) in advanced (8-day to 10-day) tumors. None of the differentiation markers were expressed, even in the most advanced stage tumors (Figure S1). Instead they exhibited high expression-levels of genes that prevent differentiation in normal myoblasts (e.g. Him, Figure S1A,E) [8, 19]. The ability of the mesenchymal cells to sustain tumor growth may therefore rely on them remaining undifferentiated.

Mesenchymal Notch activity sustains tumor growth.

Under normal conditions, Notch activity is important for preventing differentiation of the muscle progenitors [7, 20]. To evaluate Notch activity in *EGFR-psq*^{RNAi} tumors, we first made use of a reporter containing an auto-regulatory enhancer from the *Notch* gene **(***Notch[NRE]-GFP; [21]***)** which is widely responsive to Notch activity including in the muscle progenitors (marked by Cut or Twist; Figure 1E-E' and Figure S2 A-A''). In *EGFR-psq*^{RNAi} tumors *Notch[NRE]-GFP* expression was robustly up-regulated throughout the mesenchymal cells (Figure 1F-F'' and Figure S2 B-B') indicating that Notch activity is maintained in these cells during tumor growth.

Second we analyzed expression of *m6-GFP*, a Notch-responsive reporter that is expressed in a limited subdomain of the wild-type mesenchyme (Figure 1G-G' and Figure S2C-C''). The more restricted *m6-GFP* expression suggests that it requires higher levels of signaling than *Notch[NRE]*. In agreement, *m6-GFP* expression expanded through the mesenchyme when exogenous Notch activity was supplied there (Figure S2 C-D'' and [22]). Thus the two reporters appear to respond to different levels of Notch activity and *m6-GFP* marks the domain where levels of Notch activity are highest. In *EGFR-psq*^{RNAi} tumors, *m6-GFP* expression was detectable in the majority of mesenchymal cells, based on analysis with two different mesenchymal markers (Cut, Figure 1G-I and Twist, Figure S2E-

G), indicating they have high levels of Notch activity. As the expression levels were not uniform, it is likely that some mesenchymal cells have higher/lower levels of Notch activity than others. Nevertheless, *m6-GFP* was active in a large proportion of tumor mesenchymal cells (Figures 1I and S2G) and the endogenous transcript was significantly up-regulated (Figure S2H). Together these data indicate that there are high levels of Notch activity in the majority of mesenchymal cells in *EGFR-psq*^{RNAi} wing discs.

To test whether Notch activity in the mesenchyme is required to sustain tumor growth, we developed tools to manipulate gene expression in mesenchymal cells, independently of the epithelial cells, using the lexA system [23]. Thus, we generated a *Notch*^{RNAi} transgene under lexA operator control (Figure S3A-D). We first confirmed functionality by directing expression in bristle cell precusors, where it produced extra bristles characteristic of reduced Notch activity (Figure S3E-F). Next, we used it to down-regulate Notch in the mesenchymal cells, using *15B03-lexA* (Figure S3A-D), where it had a striking effect on the tumors, reducing their size to almost wild type dimensions (Figure 1J-M) although apico-basal polarity was not fully restored. Thus high levels of Notch activity are necessary in the mesenchymal cells associated with *EGFR-psq*^{RNAi} tumors to sustain their growth. These results emphasise the importance of tissue interactions in tumorigenesis and indicate an oncogenic role for Notch in the tissue that is not genetically modified.

Tumorigenic epithelial cells deliver Delta ligand and activate Notch in the mesenchymal cells.

Notch activity in the mesenchyme might arise from an increase in ligand expression in the myoblasts themselves, where Delta and Serrate are expressed under wild-type conditions [24, 25], or from inter-tissue signaling using elevated ligands in the adjacent *EGFR-psq*^{RNAi} epithelial cells. The Notch protein itself is present in both the mesenchyme and the epithelial cells, in normal and tumor wing discs (Figure S4 A-B'). To investigate ligand expression, we tagged the endogenous *Delta* and *Serrate* genes with mScarlet (Delta$^{mScarlet\text{-}I}$) and sfGFP (Serrate^{sfGFP}) respectively (Figure S4). Both ligands were expressed in the disc epithelium (Figure 2A-C and Figure S4E-E'') but were almost undetectable in the myoblasts (e.g. Figure 2C). Within the epithelium, Delta was strikingly enriched in a group of epithelial cells closely adjacent to the *m6-GFP* expressing myoblasts (Figure 2C) whereas Serrate was detected at highest levels in nearby regions (Figure S4 E-E''). As *m6-GFP* responds to high levels of Notch, the localized Delta expression could explain its restricted expression if Delta activates Notch in adjacent mesenchymal myoblasts. If the same model applies to the tumors, they should exhibit high

levels of Delta in the genetically altered epithelial cells. Indeed, when Delta expression was subsequently analyzed in *EGFR-psq*^{RNAi} tumors, high levels were systematically detected in all epithelial cells (Figure 2D,G)**,** whereas Serrate exhibited more variable expression (Figure S4F-G''). The ubiquitous upregulation of Delta in the cancerous epithelium makes it a primary candidate to mediate Notch activation in tumor mesenchymal cells, although it is possible that Serrate also makes a contribution.

In agreement with the model that signaling relies on epithelial Delta, its down-regulation in the genetically modified epithelium reduced the size of tumors (Figure S4H-J and S6B)**.** Conversely, ectopic epithelial Delta expression was sufficient to induce *m6-GFP* expression in nearby myoblasts (Figure 2I-K) of otherwise normal discs. Ectopic *m6-GFP* was associated with all Delta clones where there were adjacent mesenchyme (11 Delta clones, n= 6 discs). These results support the hypothesis that, in the tumors, Notch is activated in the mesenchymal cells through Delta ligands provided by the aberrant epithelial cells**.**

Mesenchymal Notch is activated via Delta-expressing epithelial cytonemes.

As Delta is a transmembrane ligand, our model implies that epithelial cells are able to make cell-cell contacts with the mesenchymal cells. Indeed, these contacts would need to act across a range of several cell diameters, because the mesenchymal cells are often multilayered (e.g. Figure 2H) and they express *m6-GFP* even when located at a distance from the epithelial cells (Figure 2F), albeit at lower levels than the direct neighbours (Figure 2F). One possibility is that the epithelial cells extend long processes as suggested by a recent study, which detected cytonemes in *EGFR-psq*^{RNAi} tumors [26]. To investigate, we combined membrane tagged GFP (mCD8-GFP) with *EGFR-psq*^{RNAi}, so that any epithelial cell processes would be labeled with GFP, and analyzed the distribution of Delta$^{mScarlet-I}$ (Figure 3 and S5A). Live-imaging of these tumors revealed arrays of cell processes emanating from the basal side of epithelial cells (Figure 3A-B, S5A), many of which contained multiple Delta$^{mScarlet-I}$ puncta (Figure 3B'). We refer to these as cytonemes, in accordance with [26]. In fixed tissues, Delta$^{mScarlet-I}$ puncta were detected between Twist-expressing mesenchymal cells (Figure 3C-D'), often with an interdigitated distribution resembling a cell process, although GFP-labelled cytonemes can't be visualized in fixed tissues [27]. As the Notch receptor is present in both populations (Figure S4A-B), we cannot distinguish whether there are reciprocal Notch containing processes emanating from the mesenchyme. However, it has been reported that cytonemes are also present on mesenchymal cells in these tumors [26].

Our data suggest that Delta-expressing epithelial cytonemes might sustain high levels of Notch activity in the mesenchymal cells of tumors, as reported previously for signaling to air sac cells [15]. To investigate, we depleted *Diaphanous (Dia),* an actin binding protein essential for cytoneme development [15, 28]*,* in the *EGFR-psq*^{RNAi} epithelial cells and monitored effects on *m6-GFP*, as an indicator of Notch activity (Figure 3E-I). In agreement with a recent study [26], epithelial depletion of *Dia* significantly reduced the size of the *EGFR-psq*^{RNAi} tumors (Figure 3 E and G). Importantly, *m6-GFP* expression in the mesenchymal cells was strongly decreased in comparison to control tumors (Figure 3F',H' and I). Altogether, these data provide evidance that Delta-expressing epithelial cells activate Notch in mesenchymal cells via cytonemes, to promote tumor development.

Long range signaling by Delta-containing cytonemes has been reported in some contexts [15, 29], but what the real-time response from such small, and potentially transient, interactions might be is unclear. We therefore generated a cell culture system where we could visualize the transcriptional activity of a direct Notch target when exposed to Delta-expressing cells. To do so we utilized the MS2-MCP system, whereby nascent transcripts containing MS2 loops are detected by the recruitment of GFP-tagged MS2 binding protein, MCP-GFP [30]. We first inserted 24 MS2 stem-loops and the coding sequence of LacZ into the endogenous Notch-regulated *E(spl)mβ* gene [31], using CRISPR/Cas9 genome engineering in the context of a stable cell line expressing MCP-GFP (Figure 4A-B). When Notch was activated using a chemical treatment, strong MCP-GFP puncta could be detected in the nuclei of these "Notch reporter cells" within 10-15 minutes (Figure S5B-D), in agreement with previous reports showing that *E(spl)* genes can be activated within this short timeframe [32].

We then asked how rapidly these cells responded when added to a culture of Delta-expressing cells [33]. Strikingly we could detect a clear response after 15-20 minutes despite the fact that, in many cases, the responding cells were only in contact with ligand-expressing cells through fine processes (Figure4C-G and Video S1). No transcription occurred in isolated cells or in the absence of Delta cells. Thus, Notch is effectively and rapidly activated in the reporter cells despite that they are only interacting with ligand-expressing cells through fine cellular processes, although further experiments would be required to prove unequivocally that these processes mediate contact-dependant signaling rather than exosomes or some mode of ligand presentation. Nevertheless these results harmonize with the model that cytonemes confer Delta activation from the epithelial cells to the mesenchyme in the tumors.

Notch activity promotes mitosis and prevents differentiation of mesenchymal cells.

In *EGFR-psq*^{RNAi} tumors, the mesenchymal and epithelial cells proliferate extensively. Indeed the proportions of cells containing phosphorylated histone H3 (PH3), indicative of cells undergoing mitosis, were similar between epithelial and mesenchymal tissues (Figure S6A and [4]). As Notch activity is important for proliferation and maintenance of the muscle precursors under normal conditions [7, 34, 35] we asked whether it performs a similar role in the tumor mesenchyme. First we analyzed the relative proportions of mitotic cells in domains with robust *m6-GFP* expression, indicative of high levels of Notch activity, compared to other regions (Figure 5A-C). A greater proportion of *m6-GFP* expressing cells in *EGFR-psq*^{RNAi} tumors contained pH3 than non-expressing mesenchymal cells, signifying that Notch activity promotes cell division (Figure 5B,C). The percentages of mitotic cells were also much higher than in control discs (Figure 5A,C)**.** Second, we depleted *Notch* in the mesenchymal cells. This resulted in a significant decrease in the number of mitotic cells as well as a reduction in cell numbers and tumor size (Figure 5D-G and Figure S6A). Notably, the tumors contained almost equal proportions of epithelial and mesenchymal cells wheres, when Notch was depleted in the mesenchyme, the relative size of the mesenchymal compartments was smaller and more similar in proportions to wild-type (Figure S6B). Together, these data support the idea that Notch activity contributes to the proliferation of mesenchymal cells, sustaining tumor progression.

Second, we investigated whether Notch is required in the mesenchymal cells to prevent their differentiation. Normally, the muscle differentiation program is triggered by a decline in Notch activity and in the levels of its targets, Twist and Him, which allows Mef2 levels to increase [8, 19, 36]. *EGFR-psq*^{RNAi} tumors have signatures of undifferentiated mesenchyme, with high levels of *Him* mRNA and low levels of Mef2, indicating that these cells are undifferentiated. (Figure S1). In contrast, when *Notch* was depleted in the mesenchyme, using RNAi, markers of muscle differentiation, such as Tropomyosin (Tm), were present in some mesenchymal cells (Figure S7A,B). Thus Notch activity in the mesenchymal cells inhibits their differentiation, as well as fostering their proliferation, enabling their expansion in the *EGFR-psq*^{RNAi} tumors.

Given that Dpp activity in the mesenchyme is also required to sustain *EGFR-psq*^{RNAi} tumors [4], we asked whether this was also dependent on Notch activity. However, there was no change in the levels of phosphorylated Mad (pMad), a measure of Dpp pathway activity, when *Notch* was depleted in the mesenchyme of *EGFR-psq*^{RNAi} tumors (Figure S6C-D). Likewise, when *Mad* was depleted from the mesenchyme of tumors, epithelial

Delta expression remained high, similar to control tumors (Figure S6E-F). Together these data indicate that the effect of Notch on mesenchymal cells differentiation is not via Dpp signaling but rather the two pathways are acting in parallel to regulate tumor growth.

Zfh1/ZEB acts downstream of Notch and promotes tumor growth.

The transcription factor Zfh1/ZEB is required for maintaining the myogenic progenitors and is directly regulated by Notch activity [9, 37]. As a first step to test whether Zfh1 expression contributes to Notch regulated expansion in tumors, we analyzed expression from the *zfh1* Notch responsive enhancer (Enh3-GFP). Robust *Enh3-GFP* expression was present throughout the majority of mesenchymal cells in the tumors (Figure 6A-B). In contrast, a mutated version, *Enh3[mut]-GFP,* lacking the Notch responsive motifs [9] exhibited very little, if any, expression in tumors of a similar age (Figure 6D-E'). Furthermore, there was a significant increase in the levels of both *zfh1* mRNA isoforms in tumors, compared to wild type (Figure S7). In situ hybridization and analysis of *zfh1-short*-GFP expression, confirmed that *zfh1-short,* the isoform implicated in maintaining progenitor status [9], was significantly upregulated (Figure S7). These data demonstrate that *zfh1* mRNAs, including *zfh1-short*, are highly expressed in the tumors and suggest that this occurs by direct Notch regulation via Enh3.

Given that *zfh1* levels were elevated in the mesenchymal cells, we sought to address the role of Zfh1 in tumor development. We generated strains to express $zfh1^{RNAi}$ under the control of lexAop, so that *zfh1* expression could be specifically depleted in the mesenchymal cells using the 15B03-LexA driver (Figure 6F-I). Down-regulating *zfh1* in myoblasts proved sufficient to significantly reduce tumor growth (Figure 6I and Figure S6B) and induced the premature differentiation of mesenchymal cells (Figure S7C). Similar to Notch depletion, the apico-basal organization was however not fully restored (Figure 6F-H). Nevertheless, the reduction in tumor size caused by *zfh1* depletion argues that *zfh1* has an important functional role in the mesenchymal cells to promote tumor growth and maintenance.

DISCUSSION

Normal tissue mesenchymal cells are thought to have important roles in promoting the growth and metastasis of many tumors. To do so they must be educated by the aberrant cancerous cells to acquire the properties needed to sustain tumorigenesis. Using a *Drosophila* model of EGFR/Ras-driven tumorigenesis [4, 17] we demonstrate that Notch activity in the unmodified mesenchymal cells is essential for tumor growth. Down-regulating Notch specifically in mesenchymal cells reduced their proliferation rates, promoted their differentiation and significantly compromised the size of tumors that developed. Strikingly, the activation of Notch in these supporting cells appears to rely on direct communication from the cancerous epithelial cells, illustrating that this pathway can operate in long-range signaling between tissue layers (Figure 7).

The conclusion that Notch receptors in the mesenchymal cells are activated from ligands presented by nearby epithelial cells is unexpected, because most examples of Notch signaling occur between cells within an epithelial cell layer. The fact that the ligands are transmembrane proteins means that direct cell-cell contacts are required to elicit signaling, and that signaling usually occurs between neighboring cells. More recently, examples have emerged where signaling occurs across longer distances that appear to involve contacts mediated by cell protusions, such as filopodia or cytonemes [14-16]. Our evidence indicates that a similar mechanism operates in tumors. Delta is produced in the epithelial cells and can be detected in fine processes that extend through the nearby mesenchymal cells, consistent with a recent report describing cytonemes in these *EGFR-psq*^{RNAi} tumors [26]. In a heterologous system, we found there was robust activation of a Notch target gene rapidly after ligand expressing cells made contact through cell processes. Likewise, ectopic patches of Delta in the disc epithelium led to expression of the Notch-regulated *m6-GFP* in the underlying mesenchyme. Thus we propose that the widespread upregulation of Delta in the epithelial compartment of the tumorous wing discs in turn activates the Notch pathway in the neighbouring mesenchymal cells via long cellular processes. As a consequence, the mesenchymal cells become coordinated with the cancer epithelial cells and are maintained in an undifferentiated state (Figure 7).

While our data demonstrate that Delta-Notch mediated inter-tissue signaling is important for sustaining tumor growth, it is evident that other signals are also required. First, it was previously shown that Dpp from the cancerous epithelium is essential for these tumors to grow [4]. Since the Dpp pathway was still activated in the mesenchyme when Notch was depleted, we propose that Dpp and Notch operate in parallel. This may explain why

apicobasal polarity was not fully restored when Notch activity was impaired and highlights the likelihood that several different pathways are coopted to drive tumorigenesis. Second, the fact that tumorigenesis is rescued by perturbing Notch (Figure 1) or Dpp signaling [4] in the mesenchyme, argues that there must be a reciprocal signal to the epithelium. Notably, the relative growth of the two populations appears highly co-ordinated in the tumors (Figure S6B) unlike wild-type where the epithelial growth predominates. A plausible model is that combined inputs from Notch and Dpp are required to produce reciprocal signal(s) and it will be interesting to discover whether the reciprocal signaling also operates through cytonemes, given that the mesenchymal cells emit processes [26].

One of the key effectors of Notch activity in the tumor mesenchyme is Zfh1/ZEB, which is important for maintaining the muscle progenitors in normal conditions. In a similar manner, its expression is kept high in the tumor mesenchyme, due to Notch activity, where it helps prevent their differentiation. Down-regulating *zfh1* in mesenchymal cells induces their premature differentiation and prevents tumors growth. The role of Zfh1/ZEB in promoting progenitors and stem cell proliferation appears to be widespread [10]. Furthermore, ZEB1 is upregulated in many cancers, where it can cause the expansion of cancer stem cells and frequently drives epithelial to mesechymal transition to promote metastasis [38, 39]. Whether its activation in these conditions also involves Notch activation and inter-tissue signaling remains to be determined.

Acknowledgments

We thank Hector Herranz, Steve Cohen, Ruth Lehmann, Eileen Furlong the Bloomington Stock Center, the VDRC Stock Center and the Developmental Studies Hybridoma Bank for *Drosophila* strains and antibodies. We thank Julia Falo-Sanjuan, Kat Millen, Gustavo Cerda-Moya and Ismael Morin-Poulard for the technical help and data analysis. We thank other members of SJB lab for valuable discussion. HB thanks Fabienne Pituello, Michèle Crozatier and Alain Vicent for accommodating him in the Centre de Biologie du Développement while revising the manuscript. This work was funded by an MRC programme grant MR/L007177/1, an Isaac Newton Trust research grant, and a BBSRC project grant BB/P006175/1. HB was supported by EMBO Long Term (ALTF 325-2013) and AFM-Téléthon (22599) fellowships, and ZP by a studentship from BBSRC (1502069).

Authors contributions

H.B, T.M and S.J.B designed the experiments. H.B, T.M, Z.P and T.K performed the experiments. H.B, T.M, Z.P and S.J.B analysed the data. H.B and S.J.B wrote the manuscript.

Declaration of interests: The authors declare that they have no competing interests.

Main figure titles and legends

Figure 1. Requirement for Notch activity in tumor mesenchyme. (**A-B**) *Apterous-Gal4* (Green, *ap-Gal4>UAS-mCD8::GFP*) drives expression in epithelial cells but not myoblasts (Twist, Magenta). (**B**) Optical cross-sections of A demonstrate that the epithelium (E) and myoblasts (M) form separate tissue-layers. (**C-D**) Tumors induced by expression of *EGFR* and psq^{RNAi} *(ap-Gal4>UAS-EGFR;UAS-*psq^{RNAi}*)* co-expressing mCD8::GFP, 8 days after induction; epithelial (Green) and mesenchymal cells (Magenta) become intermingled. (**C'**) Higher magnification (6x) of boxed region in C. (**D**) Optical cross-sections of C'. (**E-F**) Expression of *Notch[NRE]-GFP* reporter (Green) in wild type myoblasts (**E-E'**: Cut, Magenta) and in mesenchyme of *ap>EGFR-*psq^{RNAi} tumors (**F-F'')**. DE-Cadherin (DE-Cad), blue, marks epithelial cells. (**G-H'**) Expression of *m6-GFP* reporter (green) is detected in a small group of myoblasts (Cut, Magenta) in wild type (**G-G'**) but is widely upregulated throughout the mesenchyme (Cut, Magenta) in *ap>EGFR-*psq^{RNAi} tumors (**H-H'''**). DE-Cad, blue, marks epithelial cells. G' and H''' are optical cross-sections**.** (**I**) Proportion of myoblasts expressing *m6-GFP* in the indicated genotypes (****p<0.0001, unpaired t-test; n=18 wild type, n=22 tumorous wing discs; light, dark and intermediate shading indicates data points from three independent replicates). (**J-L**) Depletion of Notch in mesenchymal cells reduces tumor size. **(J)** Wild-type disc, (**K)** *ap>EGFR-*psq^{RNAi} tumor (**L**) *ap>EGFR-*psq^{RNAi} tumor after mesenchymal Notch depletion with *15B03-lexA; LexAop-*$Notch^{RNAi}$*.* DE-Cad (green) marks epithelial cells and Cut (magenta) marks the myoblasts/mesenchyme. (**M**) Volumes in the indicated genotypes (****p<0.0001; Mann–Whitney *U* test, n=27 wing discs from each genotype; light, dark and intermediate shading indicates data points from three independent replicates). Scale bars represent 100μm. See also Figure S1, S2,S3 and Table S1.

Figure 2. Tumorigenic epithelial cells provide Delta to activate Notch in nearby mesenchymal cells. (**A-C**) Delta is enriched in a patch of epithelial cells adjacent to *m6-*

GFP expressing myoblasts; normal wing disc with Delta (*Delta*$^{mScarlet-I,}$ Magenta) and *m6-GFP* (Green) expression in notal region, Twist, (blue) marks myoblasts. (**D-F**) In *ap>EGFR-psq*^{RNAi} tumors, high levels of Delta (Delta, magenta) are detected in epithelial cells but not mesenchyme *(*Twist, Blue), where *m6-GFP* is up-regulated (GFP, green). (**E-F**) Individual channels of boxed region in D. *m6-GFP* expression is elevated in mesenchymal cells adjacent to the epithelial cell layers. (**G-G'**) Apical confocal plan of *ap>EGFR-psq*^{RNAi} tumors expressing *Delta*$^{mScarlet-I}$, Twist (Green) marks mesenchyme. (**G'**) Higher magnification (10x) of boxed region in G. (**H**) Sagittal section of G' demonstrates multi-layering of mesenchymal cells which reduces proportions making direct cell contact with epithelial cells (asterisks). (**I-K**) Over-expression of Delta in epithelial clones (marked by RFP, magenta) leads to ectopic *m6-GFP* (GFP, Green) in adjacent mesenchyme (arrow; other small patches of Delta/RFP lack any adjacent mesenchyme). Rectanglular boxes (I) contain XZ and YZ sections in the planes indicated by the dashed axes. Dotted lines indicates the morphological boundary separating epithelium and mesenchyme. **J-K**) Higher magnification (25x) of sections in (I) corresponding to the region indicated by the intersection of the dashed axes, with epithelial (E) mesenchyme (M) layers. Scale bars represent 50μm. See also Figure S4 and Table S1.

Figure 3. Epithelial cells signal via cytonemes to activate Notch in the mesenchymal cells. (**A-B'**) Long cell processes, cytonemes, (*mCD8::GFP*, Green), extend from the basal side of epithelial cells in *ap>EGFR-psq*^{RNAi} tumors. Scale bars: 10μm. (**B'**) Higher magnification of boxed region in B, Delta (Delta$^{mScarlet-I}$, Magenta) puncta can be detected along the cytonemes. Scale bar: 5μm. (**C-D'**) Delta puncta (Delta$^{mScarlet-I}$, magenta) are detected along the boundary between mesenchymal cells (Twist, green) in *ap>EGFR-psq*^{RNAi} tumors, DAPI (blue) marks all nuclei. (**D-D'**) Higher magnification of boxed region in C: Delta$^{mScarlet-I}$ puncta are in close association with mesenchyme (arrowheads in D'). Scale bars represent 10μm. (**E-I**) Impairement of epithelial cytonemes, via *Dia* depletion (G-H), prevents tumor growth and reduces mesenchymal Notch activity (*m6-GFP*, Green; Cut, Magenta). DAPI (blue) marks all nuclei. (**E-F')** High levels of *m6-GFP* (Green) in mesenchyme of *ap> EGFR-psq*^{RNAi} tumors; (F-F') higher magnification of boxed region in E. (**G-H'**) Ablating cytonemes by expressing *Dia*^{RNAi} in epithelial cells reduces *m6-GFP* in the mesenchyme; *(H-H')* higher magnification of boxed region in G. **(I)** Proportions of myoblasts expressing *m6-GFP* in the indicated genotypes (**** p<0.0001; Mann–Whitney *U* test, n=21 *EGFR-psq*^{RNAi} (Control), n=20 *EGFR-psq*^{RNAi} + *dia*^{RNAi}. Light, dark and

intermediate shading indicates data points from three independent replicates). See also Figure S5 and Table S1.

Figure 4. Live imaging of transcriptional response to ligand-expressing cells. (**A-B**) Scheme illustrating strategy for MS2 tagging of *E(spl)mβ-HLH* gene. (**A**) Modified *E(spl)mβ* transcripts contain *MS2* stem-loops (mβ-MS2) which are bound by the MCP-GFP, producing nuclear puncta when *E(spl)mβ* is active. (**B**) Schematic for genome editing of *E(spl)mβ* with CRISPR/Cas9 to insert 24 *MS2 stem-loops* (MS2SL) and *lacZ* coding sequences along with a blasticidin resistance cassette ($Blast^R$) flanked by FRT sites. Similar results were obtained with and without removal of $Blast^R$. (**C**) Cellular projections emanate from both S2-Delta (α-Delta, Magenta) and *mβ-MS2* cells (GFP, Green, arrows). (**D-F**) Time course (mins) demonstrating that transcription foci (MCP puncta, white) are detected in nuclei of *mβ-MS2* cells 15-20 minutes after mixing with S2-Delta cells, when cellular process are seen extending between the cells (arrows in D; note S2-Delta cells do not express any Notch receptor). (**E**) Individual track of the maximum *mβ-MS2* transcriptional fluorescence intensity of the cell nucleus indicated in **D**. (**F**) Time course with mean maximum fluorescence for all responding mβ-MS2 nuclei following exposure to S2-Delta cells, (error bars indicate s.e.m, n=16). (**G**) No transcriptional response was detected in experiments where *mβ-MS2* cells were incubated without S2-Dl cells. See also Figure S5, Video S1 and Table S1.

Figure 5. High Notch activity in the mesenchymal tumor cells sustains their proliferation. (**A-B''**) Mitotic cells (anti-PH3, blue) in wild type (A) and *ap>EGFR-psq*^{RNAi} tumors (B) samples, Twist (magenta) marks all mesenchymal cells and *m6-GFP* (green) indicates Notch activity. Insets in B'-B'' are enlarged views (2X) of framed regions in B. Scale bars, 100μm. (**C**) Ratio of *m6-GFP* positive or negative myoblasts that have PH3 (****p<0.0001, unpaired t-test, light, dark shading indicates data points from two independent replicates). (**D-G**) Notch activity is required for mesenchymal-cell proliferation. Wild type discs (**D**), *ap>EGFR-psq*^{RNAi} tumors (**E**) and *ap>EGFR-psq*^{RNAi} *tumors* in which mesenchymal Notch is depleted using *15B03-lexA; LexAop-Notch*^{RNAi} (**F**) stained with anti-Twist (Magenta), anti-PH3 (Green) and DAPI (Blue). (**G**) Quantification of myoblast mitotic index in the conditions shown in **D,E** and **F*****, p<0.0001 (Mann–Whitney *U* test). Light, dark shading indicates data points from two independent replicates. Scale bars: 100μm. See also Figure S6 and Table S1.

Figure 6. Zfh1/ZEB is directly regulated by Notch and is required in tumor mesenchyme. (**A-B**) Expression of *Enh3-GFP* in wild type (**A**) and *ap>EGFR-psq*^{RNAi} (**B**) discs, where its expression is greatly expanded through the mesenchyme (Cut, Magenta). (**C**) Proportion of myoblasts/mesenchyme expressing *Enh3-GFP* in the indicated genotypes (****p<0.0001, unpaired t-test, n=15 wild type and 18 *EGFR-psq*^{RNAi} wing discs, light and dark shading indicates data points from two independent replicates). Scale bars: 100μm. (**D-E'**) *Enh3* expression (**D**, *Enh3-GFP*, Green) in mesenchymal cells (Twist, Magenta) is abolished when Su(H) motifs are mutated (**E**, *Enh3[mut]-GFP*, Green). Scale bars: 50 μm. (**F-I**) Down regulation of *zfh1* in mesenchymal cells reduces tumor growth. Wild type (**F**), *ap>EGFR-psq*^{RNAi} tumor (**G**) and *ap>EGFR-psq*^{RNAi} tumor where *zfh1* is depleted with *15B03-lexA; LexAop-zfh1*^{RNAi} (**H**)*;* DE-Cad (green) marks epithelial cells Cut, (Magenta) marks mesenchyme and DAPI (Blue) labels all nuclei. (**I**) Tumor volume in the indicated genotypes (****p<0.0001, Mann–Whitney *U* test; light, dark and intermediate shading indicates data points from three independent replicates). Scale bars: 100 μm. See also Figure S7 and Table S1.

Figure 7. Model summarizing the role of Notch in mediating the tumor-stroma interactions. In *EGFR-psq*^{RNAi} tumors, the tumorogenic epithelial cells contain high levels of Delta (Red) which activates Notch in the unmodified mesenchymal cells. Delta is present on epithelial cell membranes and on long cellular processes, allowing signaling to occur over longer ranges. By activating Notch, epithelial cells hijack the mesenchymal cells, preventing their differentiation and promoting proliferation so that tumorigenesis is sustained.

STAR METHODS

LEAD CONTACT AND MATERIALS AVAILABILITY

Further information and requests for resources and reagents should be directed to, and will be fulfilled by, the Lead Contact, Sarah J Bray (sjb32@hermes.cam.ac.uk).
All strains, plasmids, and reagents generated in this study are available from the Lead Contact but we may require a completed Materials Transfer Agreement.

.

EXPERIMENTAL MODEL AND SUBJECT DETAILS

Drosophila melanogater strains and genetics

All *Drosophila melanogaster* stocks were grown on standard medium at 25°C. The following stains were used: The *EGFR-psq*^{RNAi} and *15B03-lexA* lines were provided by Hector Herranz [4], *w*^{118} as wild type (wt), *UAS-white-RNAi* as control for *RNAi* experiments (BL#35573), *Ap-Gal4* (BL#25685), *UAS-mCD8-GFP* (BL#5137), *Notch[NRE]-GFP* [21], *m6-GFP* [22], *UAS-Delta*^{30B} [40], *Enh3-GFP* and *Enh3[mut]-GFP* [9], *Him-GFP* [41], *CG9650-YFP* (CPTI#1741), *MHC-lacZ* [42], *UAS-Notch∆ECD* [43-45], *LexAop-CD8-GFP* (BL#66545), *Ptc-LexA* (BL#54926), *UAS-Dl*^{RNAi} (BL#28032), *UAS-Dia*^{RNAi} (BL#33424), *LexAop-Mad*^{RNAi} [4]. The *EGFR-psq*^{RNAi} tumors were inducted as described in [4]. The flip out clones were generated using *hs-flp;Actin5c>CD2>GAL4*,*UAS-RFP (BL*#30558). The progeny obtained from the *Flip out>RFP* X *UAS-Delta; m6-GFP* crosses were heat-shocked 1h at 37°C at late second instar larva stages and analyzed as described in the Figure 2I. See Table S1 for full genotypes of samples analyzed.

Generation of fly and cell lines

LexAop-Notch^{RNAi} and *LexAop-Zfh1*^{RNAi}

Inverted repeat fragments targeting either *Notch* or *Zfh1* were amplified using *yw* genomic DNA as template and inserted into the pJFRC19 plasmid [23] at NotI and XbaI sites (Table S2). Both resulting constructs were inserted into an AttP site located at 68A4 on chromosome III by injection into *nos-phiC31-NLS; attP2* embryos. Knock down efficiency for *Notch*^{RNAi} was verified by driving the RNAi with *Ptc-LexA* and assessing the scutellar bristles phenotype (Figure S3E-F) and for *LexAop-Zfh1*^{RNAi} by assessing premature differentiation of the myoblasts with *15B03-LexA* (Figure S6C).

Dl$^{mScarlet-I}$*, Ser*^{sfGFP} *and Zfh1-Short*^{sfGFP}

Lines were generated by CRISPR-mediated homology repair (HR) strategy. For Delta$^{mScarlet-I}$**,** mScarlet-I DNA fragment was inserted at the KGAS//GGPG position, as previously described in [46]. The homology arms were cloned into a modified donor template plasmid pScarlessHD-sfGFP-DsRed (Addgene #80811), where the sfGFP was

replaced by mScarlet-I [47] using Gibson assembly strategy. Serrate^{sfGFP} was generated by inserting sfGFP at the PPS//SGD position. The homology arms were cloned into the donor template plasmid pScarlessHD-sfGFP-DsRed (Addgene #80811) using Gibson assembly. A Similar strategy was used to generate Zfh1Short^{sfGFP}, where a sfGFP was inserted at the 3' end of the first *zfh1-RA* exon. The guides RNAs were cloned into the guide RNA expression vector pCFD3 vector (Addgene #49410) [48]. The guide RNA and the donor template constructs specific for each line were injected into nos-*Cas9* (BL54591) embryos. Flies with insertions were identified by the expression of the Ds-Red in the eyes and verified by genomic PCR sequencing. The transposable element containing the DsRed was removed subsequently using the PiggyBac Transposase system.

Generation of the mβ-MS2 cell line

A cell line expressing MCP-GFP constitutively was first created by transfecting Kc167 cells (DGRC) with an MCP-GFP plasmid, generated by cloning MCP-GFP (from pMS2-GFP, Addgene #27121) [49] into the Ac5-STABLE2-neo plasmid (Addgene #32426) [50] at XbaI and HindIII sites. A single clone was subsequently isolated and amplified from the transfected cells, to ensure relatively uniforms levels of MCP-GFP expression. DNA encoding *MS2* stem-loops was inserted into the into the *E(spl)-mβ-HLH* gene (Figure 4) of the MCP-GFP cells, by CRISPR gene editing. The guide RNA expression vector was generated by inserting specific *E(spl)-mβ-HLH* oligonucleotides (Table S2) into the pCFD3 plasmid (Addgene #49410) at BbsI site. For homology directed repair, a fragment carrying two homology arms (HR), the MS2 stem-loops and a 3-kilobase region of the *lacZ* gene was inserted into plasmid pMH3 (Addgene #52528) [51] (Figure 4). The CRISPR mixture containing the gRNA, HR-MS2-LacZ and pAct-Cas9 (Addgene #62209) [48] plasmids was transfected into MCP-GFP cells. The resulting mβ-MS2 cells were selected by their resistance to the Blasticidin antibiotic and genotyped by sequencing of the modified genomic fragments. The blasticidin resistance cassette was removed by flippase-induced recombination induced with the pMH5 plasmid (Addgene #52531) [51].

METHOD DETAILS

Immunostainings and *in situ* hybridization

The following primary antibodies were used for Immunofluorescence staining: Goat anti-GFP (1:200, Abcam, ab6673), Mouse anti-Cut (1:20, DSHB), Rat anti-DE-Cad2 (1:200,

DSHB), Mouse anti-Delta (1:50, DSHB), Mouse anti-β-Gal (1:1000, Promega, Z378A), Rat anti-Tropomyosin (1:1000, Abcam, ab50567), Rabbit anti-Zfh1 (1:5000, a gift from Ruth Lehmann, New York, USA), Rabbit anti-Mef2 (1:200) and Rabbit anti-Twist (1:2000) (Gifts from Eileen Furlong, Heidelberg, Germany), Mouse anti-pH3 (1:100, Cell Signaling Technology, #9706), Mouse Anti-NICD (1:100, DSHB). *In situ* experiments were carried out according to Stellaris-protocols and as described in [9].

Quantitative RT PCR

30 to 40 Wing discs from each condition were dissected and RNA isolated using TRIzol (Life technologies). RNA was reverse transcribed using M-MLV reverse transcriptase (Promega M531A). Quantitative PCR was performed using LightCycler 480 SYBR Green I Master PCR kit (Roche 04707516001). Three independent biological replicates were analyzed for each condition. Values were normalized to the level of *Rpl32* or *Twi* (Table S2).

Cell culture experiments and imaging

In control experiments, Notch was activated by treating the cells with 4mM EGTA as described [52]. For co-culture experiments, around 2 million S2-Dl cells (which express Delta under the control of a metallothionein promoter, DGRC #152; [33] were first plated in a cell culture dish previously treated with 0.01% poly-L-lysine. Delta expression was induced with media containing 5mM of copper sulphate 24 hours before imaging. The Delta induction media was replaced by 1 million mβ-MS2 cells. The cell imaging was performed with a Leica TCS SP8 confocal microscope; the transmitted light was used alongside the GFP fluorescence to visualise the S2-Dl cells, distinguished from the GFP-expressing mβ-MS2 cells.

QUANTIFICATION AND STATISTICAL ANALYSIS

Image and statistical analysis

Samples were imaged with TCS SP8 microscopes (CAIC, University of Cambridge) at 20X or 40X magnification and 1024/1024 pixel resolutions. Live imaging experiments of the wing discs were performed as described in [53]. Image J software was used to analyze images and measure reporter expression area [54]. For experiments to compare and measure the reporter expression area, samples were prepared and analyzed in parallel, with identical conditions and the same laser parameters used for image acquisition. For

each confocal stack a similar Sum slices projections was generated using Image J software. The percentage of cells expressing the reporter was obtained by calculating (automatically) for each sample the total myoblasts area (based on myoblasts Twist or Cut markers), and the area of the GFP expression. Tissues volume (in μm^3) were measured using Volocity 3D Image analysis software (PerkinElmer). The mitotic index was calculated by dividing the total number of Myoblasts (Twist +) by the number of the cells undergoing mitosis (PH3 +). Statistics were calculated with GraphPad Prism and, depending on the Gaussian distribution of the values, either the unpaired *t* test or the Mann–Whitney non-parametric test was used as indicated in the legends.

MS2 computational analysis

Maximum projections of the videos were made using Fiji software and cells were segmented and tracked over the time with a MATLAB script (available at https://github.com/juliafs93/MS2_cells). Briefly, cells were segmented from the MCP-GFP signal using a combination of median filtering and identification of circular shapes using the "imfindcircles" function. Cells were tracked over the time by finding the closest neighbour in a 15-pixel radius and allowing search in the previous 5 frames. Tracks containing fewer than 360 frames (~1 hour) were removed from the analysis. Tracked cells were overlaid with the MCP-GFP signal to obtain the maximum intensity pixel for each nucleus, which was used as a proxy of the transcriptional spot fluorescence. This analysis provided values of maximum fluorescence for each tracked cell over time. Final fluorescent traces were obtained by applying a moving average of 5 frames and background was removed using a regression line calculated using the lower quartile of values for each cell. All traces from active cells were manually curated and in co-culture experiments t=0 was set when each *mβ-MS2* cells contacted the plate.

DATA AND CODE AVAILABILITY

The MATLAB scripts for tracking and analysing *mβ-MS2* transcription are availble at https://github.com/juliafs93/MS2_cells.

Video S1. Notch pathway is activated rapidly through long cellular processes. Related to Figure 4. Live imaging of *E(spl)mβ*-MS2 (mβ-MS2) cells co-cultured with Delta-expressing S2 cells (S2-Dl). The mβ-MS2 and S2-Dl cells make contact through long cell processes. Upon contact, transcriptional foci are visible in mβ-MS2 cells.

REFERENCES

1. Bussard, K.M., Mutkus, L., Stumpf, K., Gomez-Manzano, C., and Marini, F.C. (2016). Tumor-associated stromal cells as key contributors to the tumor microenvironment. Breast Cancer Res *18*, 84.
2. Hynes, N.E., and Lane, H.A. (2005). ERBB receptors and cancer: the complexity of targeted inhibitors. Nat Rev Cancer *5*, 341-354.
3. Chandler, C., Liu, T., Buckanovich, R., and Coffman, L.G. (2019). The double edge sword of fibrosis in cancer. Transl Res *209*, 55-67.
4. Herranz, H., Weng, R., and Cohen, S.M. (2014). Crosstalk between epithelial and mesenchymal tissues in tumorigenesis and imaginal disc development. Curr Biol *24*, 1476-1484.
5. Gunage, R.D., Dhanyasi, N., Reichert, H., and VijayRaghavan, K. (2017). Drosophila adult muscle development and regeneration. Semin Cell Dev Biol *72*, 56-66.
6. Chaturvedi, D., Reichert, H., Gunage, R.D., and VijayRaghavan, K. (2017). Identification and functional characterization of muscle satellite cells in Drosophila. Elife *6*.
7. Krejci, A., Bernard, F., Housden, B.E., Collins, S., and Bray, S.J. (2009). Direct response to Notch activation: signaling crosstalk and incoherent logic. Sci Signal *2*, ra1.
8. Bernard, F., Krejci, A., Housden, B., Adryan, B., and Bray, S.J. (2010). Specificity of Notch pathway activation: twist controls the transcriptional output in adult muscle progenitors. Development *137*, 2633-2642.
9. Boukhatmi, H., and Bray, S. (2018). A population of adult satellite-like cells in Drosophila is maintained through a switch in RNA-isoforms. Elife *7*.
10. Siles, L., Ninfali, C., Cortes, M., Darling, D.S., and Postigo, A. (2019). ZEB1 protects skeletal muscle from damage and is required for its regeneration. Nat Commun *10*, 1364.
11. Gascard, P., and Tlsty, T.D. (2016). Carcinoma-associated fibroblasts: orchestrating the composition of malignancy. Genes Dev *30*, 1002-1019.
12. Chen, W.J., Ho, C.C., Chang, Y.L., Chen, H.Y., Lin, C.A., Ling, T.Y., Yu, S.L., Yuan, S.S., Chen, Y.J., Lin, C.Y., et al. (2014). Cancer-associated fibroblasts regulate the plasticity of lung cancer stemness via paracrine signalling. Nat Commun *5*, 3472.
13. Bray, S.J. (2016). Notch signalling in context. Nat Rev Mol Cell Biol *17*, 722-735.
14. Cohen, M., Georgiou, M., Stevenson, N.L., Miodownik, M., and Baum, B. (2010). Dynamic filopodia transmit intermittent Delta-Notch signaling to drive pattern refinement during lateral inhibition. Dev Cell *19*, 78-89.
15. Huang, H., and Kornberg, T.B. (2015). Myoblast cytonemes mediate Wg signaling from the wing imaginal disc and Delta-Notch signaling to the air sac primordium. Elife *4*, e06114.
16. Eom, D.S., Bain, E.J., Patterson, L.B., Grout, M.E., and Parichy, D.M. (2015). Long-distance communication by specialized cellular projections during pigment pattern development and evolution. Elife *4*.
17. Eichenlaub, T., Villadsen, R., Freitas, F.C.P., Andrejeva, D., Aldana, B.I., Nguyen, H.T., Petersen, O.W., Gorodkin, J., Herranz, H., and Cohen, S.M. (2018). Warburg Effect Metabolism Drives Neoplasia in a Drosophila Genetic Model of Epithelial Cancer. Curr Biol *28*, 3220-3228 e3226.
18. del Valle Rodriguez, A., Didiano, D., and Desplan, C. (2011). Power tools for gene expression and clonal analysis in Drosophila. Nat Methods *9*, 47-55.
19. Soler, C., and Taylor, M.V. (2009). The Him gene inhibits the development of Drosophila flight muscles during metamorphosis. Mech Dev *126*, 595-603.

20. Figeac, N., Jagla, T., Aradhya, R., Da Ponte, J.P., and Jagla, K. (2010). Drosophila adult muscle precursors form a network of interconnected cells and are specified by the rhomboid-triggered EGF pathway. Development *137*, 1965-1973.
21. Simon, R., Aparicio, R., Housden, B.E., Bray, S., and Busturia, A. (2014). Drosophila p53 controls Notch expression and balances apoptosis and proliferation. Apoptosis *19*, 1430-1443.
22. Lai, E.C., Bodner, R., and Posakony, J.W. (2000). The enhancer of split complex of Drosophila includes four Notch-regulated members of the bearded gene family. Development *127*, 3441-3455.
23. Pfeiffer, B.D., Ngo, T.T., Hibbard, K.L., Murphy, C., Jenett, A., Truman, J.W., and Rubin, G.M. (2010). Refinement of tools for targeted gene expression in Drosophila. Genetics *186*, 735-755.
24. Gildor, B., Schejter, E.D., and Shilo, B.Z. (2012). Bidirectional Notch activation represses fusion competence in swarming adult Drosophila myoblasts. Development *139*, 4040-4050.
25. Bernard, F., Dutriaux, A., Silber, J., and Lalouette, A. (2006). Notch pathway repression by vestigial is required to promote indirect flight muscle differentiation in Drosophila melanogaster. Dev Biol *295*, 164-177.
26. Fereres, S., Hatori, R., Hatori, M., and Kornberg, T.B. (2019). Cytoneme-mediated signaling essential for tumorigenesis. PLoS Genet *15*, e1008415.
27. Kornberg, T.B., and Roy, S. (2014). Cytonemes as specialized signaling filopodia. Development *141*, 729-736.
28. Gonzalez-Mendez, L., Seijo-Barandiaran, I., and Guerrero, I. (2017). Cytoneme-mediated cell-cell contacts for Hedgehog reception. Elife *6*.
29. De Joussineau, C., Soule, J., Martin, M., Anguille, C., Montcourrier, P., and Alexandre, D. (2003). Delta-promoted filopodia mediate long-range lateral inhibition in Drosophila. Nature *426*, 555-559.
30. Garcia, H.G., Tikhonov, M., Lin, A., and Gregor, T. (2013). Quantitative imaging of transcription in living Drosophila embryos links polymerase activity to patterning. Curr Biol *23*, 2140-2145.
31. Cooper, M.T., Tyler, D.M., Furriols, M., Chalkiadaki, A., Delidakis, C., and Bray, S. (2000). Spatially restricted factors cooperate with notch in the regulation of Enhancer of split genes. Dev Biol *221*, 390-403.
32. Housden, B.E., Fu, A.Q., Krejci, A., Bernard, F., Fischer, B., Tavare, S., Russell, S., and Bray, S.J. (2013). Transcriptional dynamics elicited by a short pulse of notch activation involves feed-forward regulation by E(spl)/Hes genes. PLoS Genet *9*, e1003162.
33. Fehon, R.G., Kooh, P.J., Rebay, I., Regan, C.L., Xu, T., Muskavitch, M.A., and Artavanis-Tsakonas, S. (1990). Molecular interactions between the protein products of the neurogenic loci Notch and Delta, two EGF-homologous genes in Drosophila. Cell *61*, 523-534.
34. Gunage, R.D., Reichert, H., and VijayRaghavan, K. (2014). Identification of a new stem cell population that generates Drosophila flight muscles. Elife *3*.
35. Aradhya, R., Zmojdzian, M., Da Ponte, J.P., and Jagla, K. (2015). Muscle niche-driven Insulin-Notch-Myc cascade reactivates dormant Adult Muscle Precursors in Drosophila. Elife *4*.
36. Anant, S., Roy, S., and VijayRaghavan, K. (1998). Twist and Notch negatively regulate adult muscle differentiation in Drosophila. Development *125*, 1361-1369.
37. Postigo, A.A., Ward, E., Skeath, J.B., and Dean, D.C. (1999). zfh-1, the Drosophila homologue of ZEB, is a transcriptional repressor that regulates somatic myogenesis. Mol Cell Biol *19*, 7255-7263.

38. Sanchez-Tillo, E., Siles, L., de Barrios, O., Cuatrecasas, M., Vaquero, E.C., Castells, A., and Postigo, A. (2011). Expanding roles of ZEB factors in tumorigenesis and tumor progression. Am J Cancer Res *1*, 897-912.
39. Hanrahan, K., O'Neill, A., Prencipe, M., Bugler, J., Murphy, L., Fabre, A., Puhr, M., Culig, Z., Murphy, K., and Watson, R.W. (2017). The role of epithelial-mesenchymal transition drivers ZEB1 and ZEB2 in mediating docetaxel-resistant prostate cancer. Mol Oncol *11*, 251-265.
40. Doherty, D., Feger, G., Younger-Shepherd, S., Jan, L.Y., and Jan, Y.N. (1996). Delta is a ventral to dorsal signal complementary to Serrate, another Notch ligand, in Drosophila wing formation. Genes Dev *10*, 421-434.
41. Rebeiz, M., Reeves, N.L., and Posakony, J.W. (2002). SCORE: a computational approach to the identification of cis-regulatory modules and target genes in whole-genome sequence data. Site clustering over random expectation. Proc Natl Acad Sci U S A *99*, 9888-9893.
42. Hess, N.K., Singer, P.A., Trinh, K., Nikkhoy, M., and Bernstein, S.I. (2007). Transcriptional regulation of the Drosophila melanogaster muscle myosin heavy-chain gene. Gene Expr Patterns *7*, 413-422.
43. Chanet, S., Vodovar, N., Mayau, V., and Schweisguth, F. (2009). Genome engineering-based analysis of Bearded family genes reveals both functional redundancy and a nonessential function in lateral inhibition in Drosophila. Genetics *182*, 1101-1108.
44. Fortini, M.E., and Artavanis-Tsakonas, S. (1993). Notch: neurogenesis is only part of the picture. Cell *75*, 1245-1247.
45. Rebay, I., Fehon, R.G., and Artavanis-Tsakonas, S. (1993). Specific truncations of Drosophila Notch define dominant activated and dominant negative forms of the receptor. Cell *74*, 319-329.
46. Corson, F., Couturier, L., Rouault, H., Mazouni, K., and Schweisguth, F. (2017). Self-organized Notch dynamics generate stereotyped sensory organ patterns in Drosophila. Science *356*.
47. Bindels, D.S., Haarbosch, L., van Weeren, L., Postma, M., Wiese, K.E., Mastop, M., Aumonier, S., Gotthard, G., Royant, A., Hink, M.A., et al. (2017). mScarlet: a bright monomeric red fluorescent protein for cellular imaging. Nat Methods *14*, 53-56.
48. Port, F., Chen, H.M., Lee, T., and Bullock, S.L. (2014). Optimized CRISPR/Cas tools for efficient germline and somatic genome engineering in Drosophila. Proc Natl Acad Sci U S A *111*, E2967-2976.
49. Fusco, D., Accornero, N., Lavoie, B., Shenoy, S.M., Blanchard, J.M., Singer, R.H., and Bertrand, E. (2003). Single mRNA molecules demonstrate probabilistic movement in living mammalian cells. Curr Biol *13*, 161-167.
50. Gonzalez, M., Martin-Ruiz, I., Jimenez, S., Pirone, L., Barrio, R., and Sutherland, J.D. (2011). Generation of stable Drosophila cell lines using multicistronic vectors. Sci Rep *1*, 75.
51. Bottcher, R., Hollmann, M., Merk, K., Nitschko, V., Obermaier, C., Philippou-Massier, J., Wieland, I., Gaul, U., and Forstemann, K. (2014). Efficient chromosomal gene modification with CRISPR/cas9 and PCR-based homologous recombination donors in cultured Drosophila cells. Nucleic Acids Res *42*, e89.
52. Pillidge, Z., and Bray, S.J. (2019). SWI/SNF chromatin remodeling controls Notch-responsive enhancer accessibility. EMBO Rep *20*.
53. Aldaz, S., Escudero, L.M., and Freeman, M. (2010). Live imaging of Drosophila imaginal disc development. Proc Natl Acad Sci U S A *107*, 14217-14222.
54. Schneider, C.A., Rasband, W.S., and Eliceiri, K.W. (2012). NIH Image to ImageJ: 25 years of image analysis. Nat Methods *9*, 671-675.

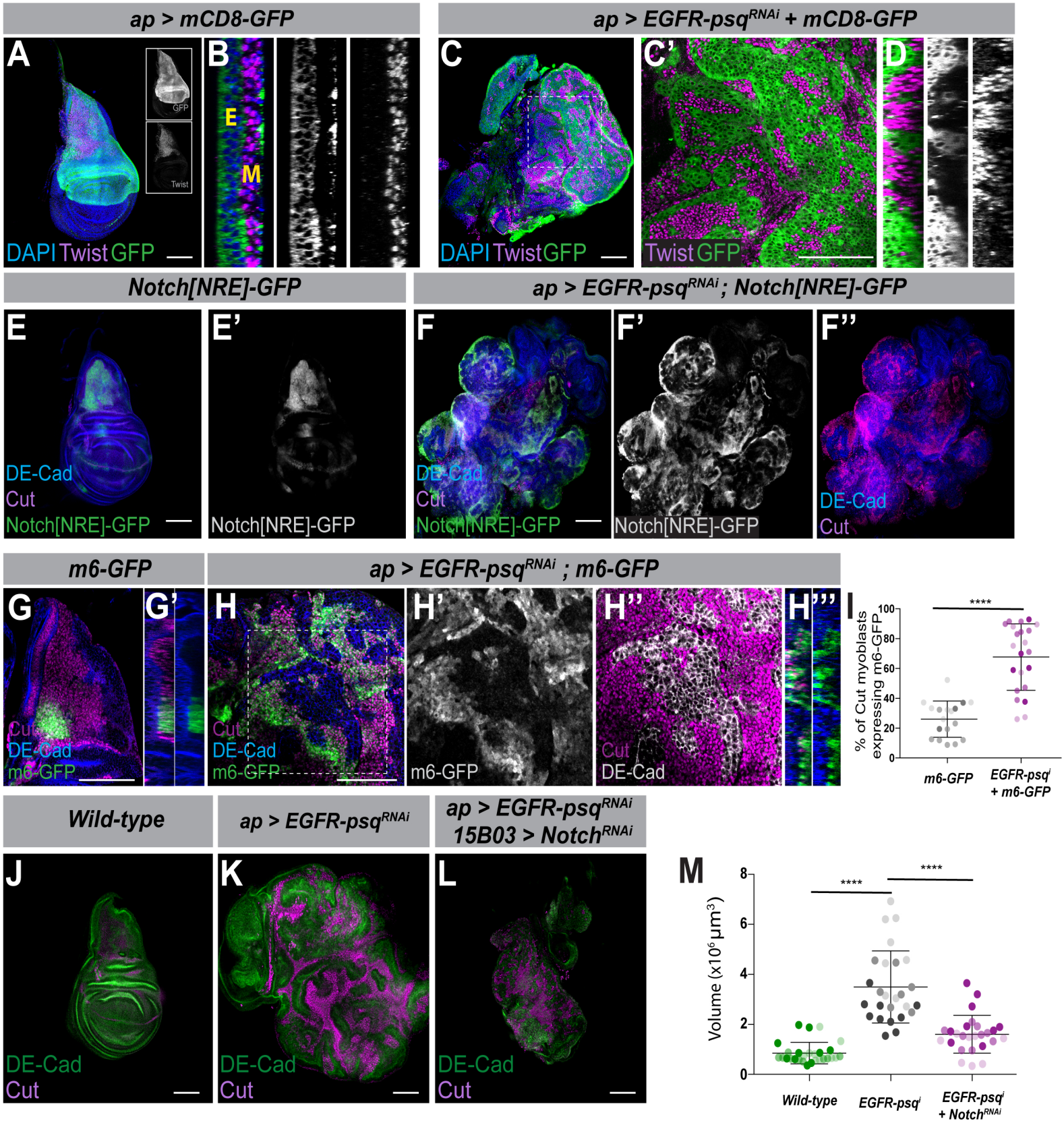
ap > mCD8-GFP
ap > EGFR-psq^RNAi + mCD8-GFP
A
B
C
C'
D
E
M
GFP
Twist
DAPI Twist GFP
Twist GFP
Notch[NRE]-GFP
ap > EGFR-psq^RNAi ; Notch[NRE]-GFP
E
E'
F
F'
F''
DE-Cad
Cut
Notch[NRE]-GFP
m6-GFP
ap > EGFR-psq^RNAi ; m6-GFP
G
G'
H
H'
H''
H'''
I
% of Cut myoblasts expressing m6-GFP
****
m6-GFP
EGFR-psq^i + m6-GFP
Wild-type
ap > EGFR-psq^RNAi
ap > EGFR-psq^RNAi 15B03 > Notch^RNAi
J
K
L
M
Volume (x10^6 µm^3)
Wild-type
EGFR-psq^i
EGFR-psq^i + Notch^RNAi

Figure 1

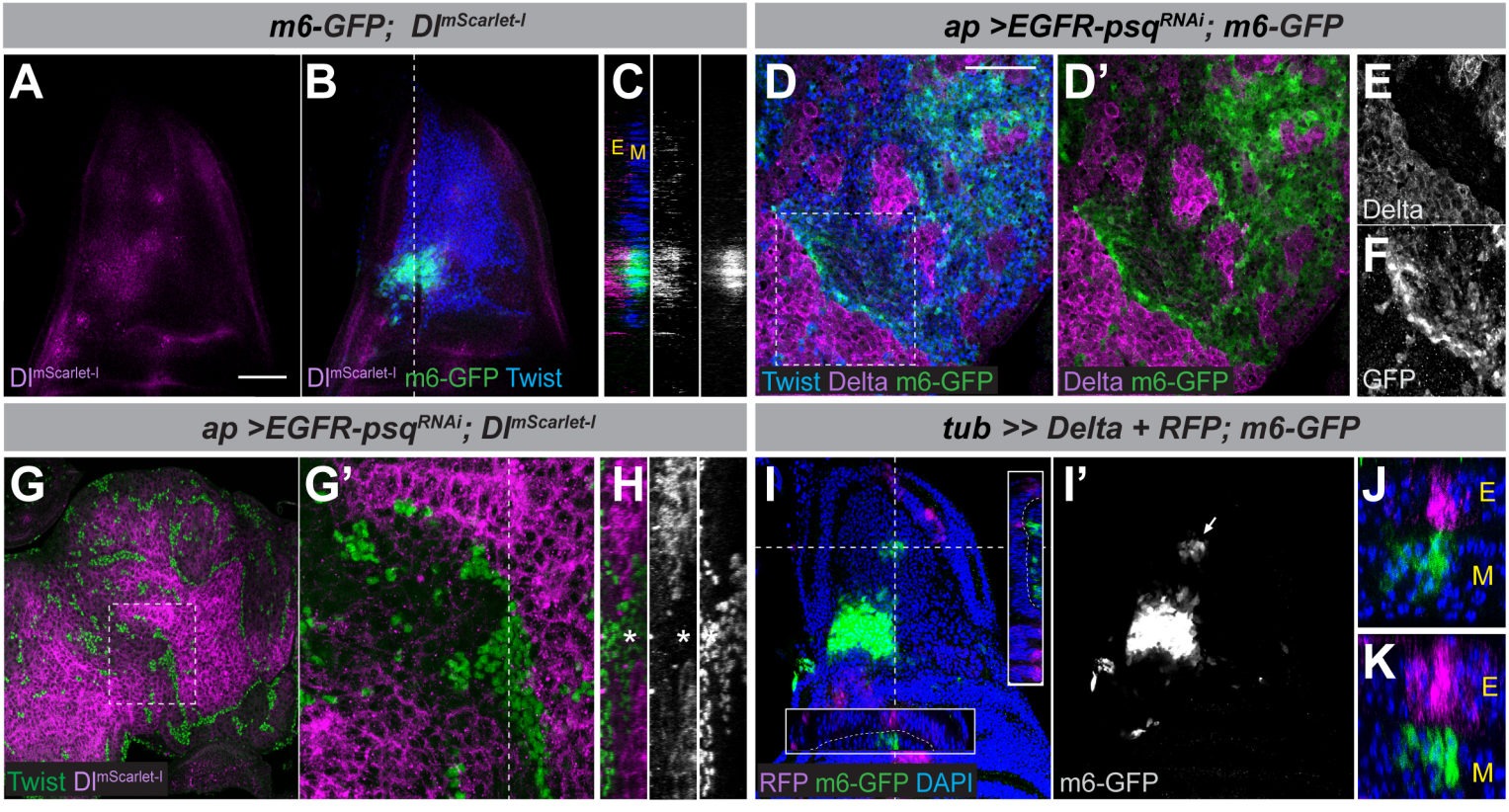
m6-GFP; Dl^mScarlet-I
ap >EGFR-psq^RNAi; m6-GFP
ap >EGFR-psq^RNAi; Dl^mScarlet-I
tub >> Delta + RFP; m6-GFP
A
B
C
D
D'
E
F
G
G'
H
I
I'
J
K
Dl^mScarlet-I
Dl^mScarlet-I m6-GFP Twist
E M
Twist Delta m6-GFP
Delta m6-GFP
Delta
GFP
Twist Dl^mScarlet-I
RFP m6-GFP DAPI
m6-GFP
E
M
E
M

Figure 2

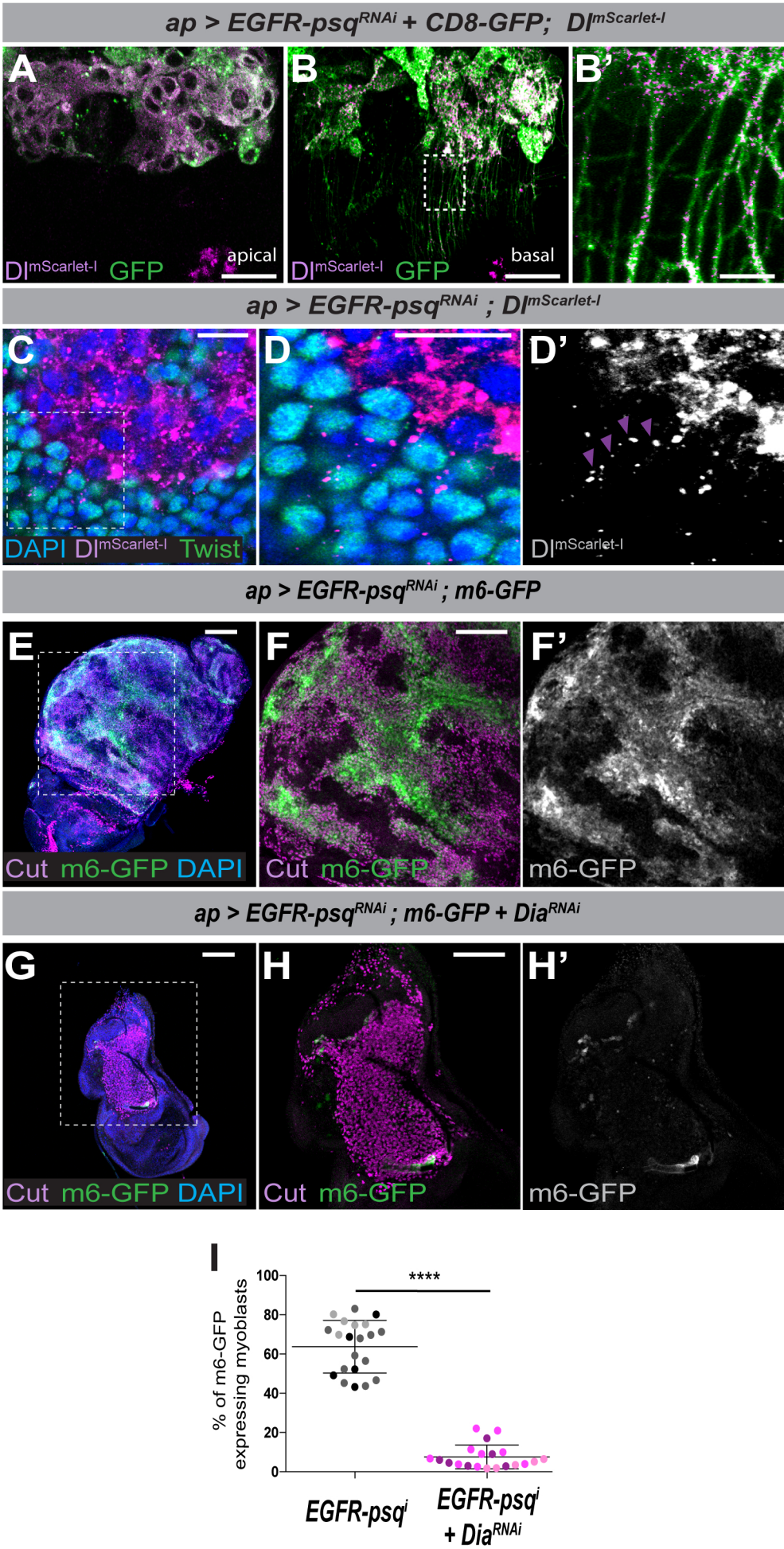
ap > EGFR-psq^RNAi + CD8-GFP; Dl^mScarlet-I
A
Dl^mScarlet-I GFP
apical
B
Dl^mScarlet-I GFP
basal
B'
ap > EGFR-psq^RNAi ; Dl^mScarlet-I
C
DAPI Dl^mScarlet-I Twist
D
D'
Dl^mScarlet-I
ap > EGFR-psq^RNAi ; m6-GFP
E
Cut m6-GFP DAPI
F
Cut m6-GFP
F'
m6-GFP
ap > EGFR-psq^RNAi ; m6-GFP + Dia^RNAi
G
Cut m6-GFP DAPI
H
Cut m6-GFP
H'
m6-GFP
I
% of m6-GFP expressing myoblasts
100
80
60
40
20
0
****
EGFR-psq^i
EGFR-psq^i + Dia^RNAi

Figure 3

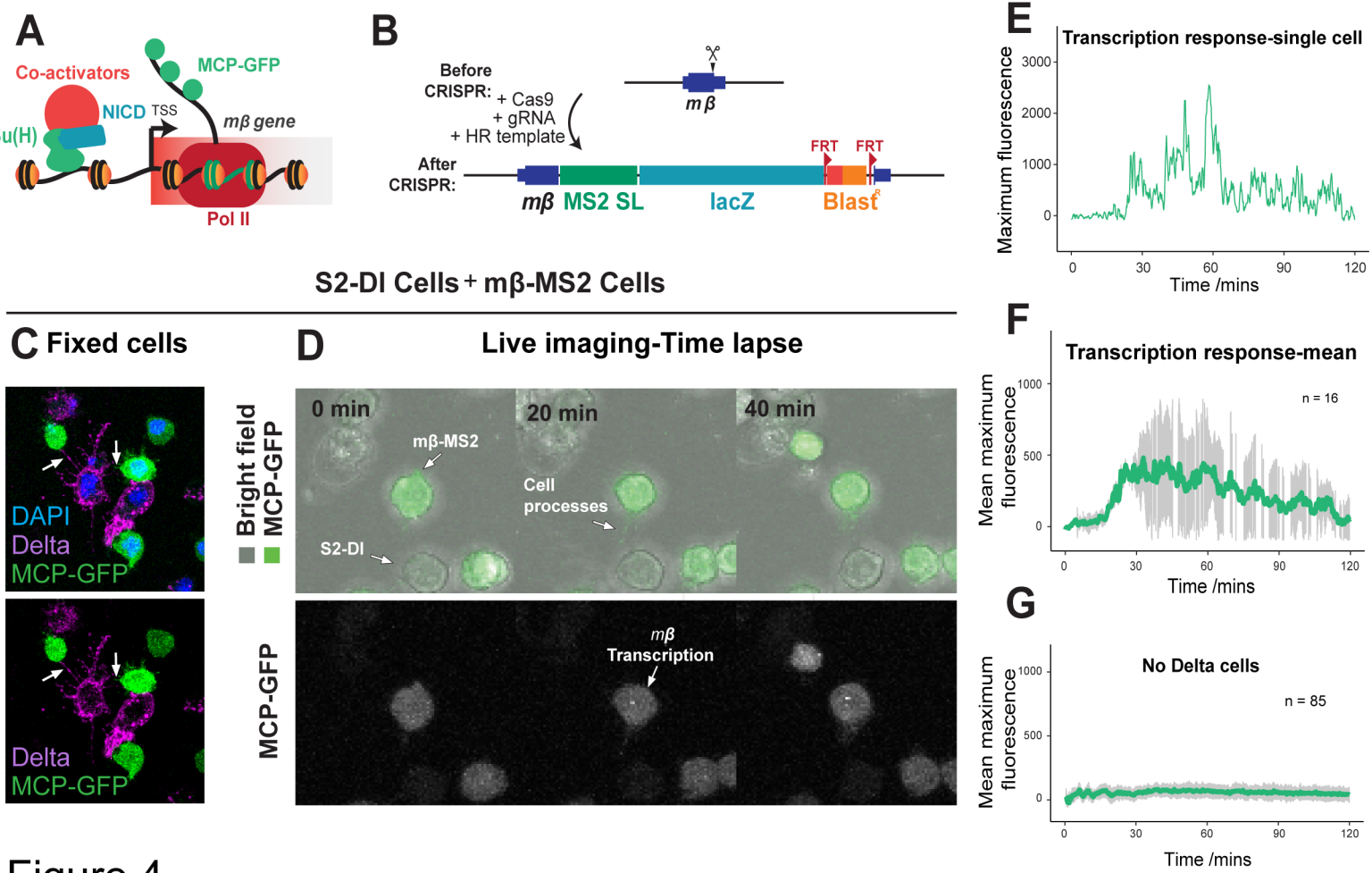
A
Co-activators
MCP-GFP
NICD
TSS
Su(H)
mβ gene
Pol II
B
Before CRISPR:
+ Cas9
+ gRNA
+ HR template
mβ
After CRISPR:
FRT
FRT
mβ
MS2 SL
lacZ
Blast
S2-DI Cells + mβ-MS2 Cells
C Fixed cells
DAPI
Delta
MCP-GFP
Delta
MCP-GFP
D
Live imaging-Time lapse
Bright field
MCP-GFP
0 min
20 min
40 min
mβ-MS2
Cell processes
S2-DI
MCP-GFP
mβ Transcription
E
Transcription response-single cell
Maximum fluorescence
3000
2000
1000
0
0
30
60
90
120
Time /mins
F
Transcription response-mean
Mean maximum fluorescence
1000
500
0
n = 16
0
30
60
90
120
Time /mins
G
No Delta cells
Mean maximum fluorescence
1000
500
0
n = 85
0
30
60
90
120
Time /mins

Figure 4

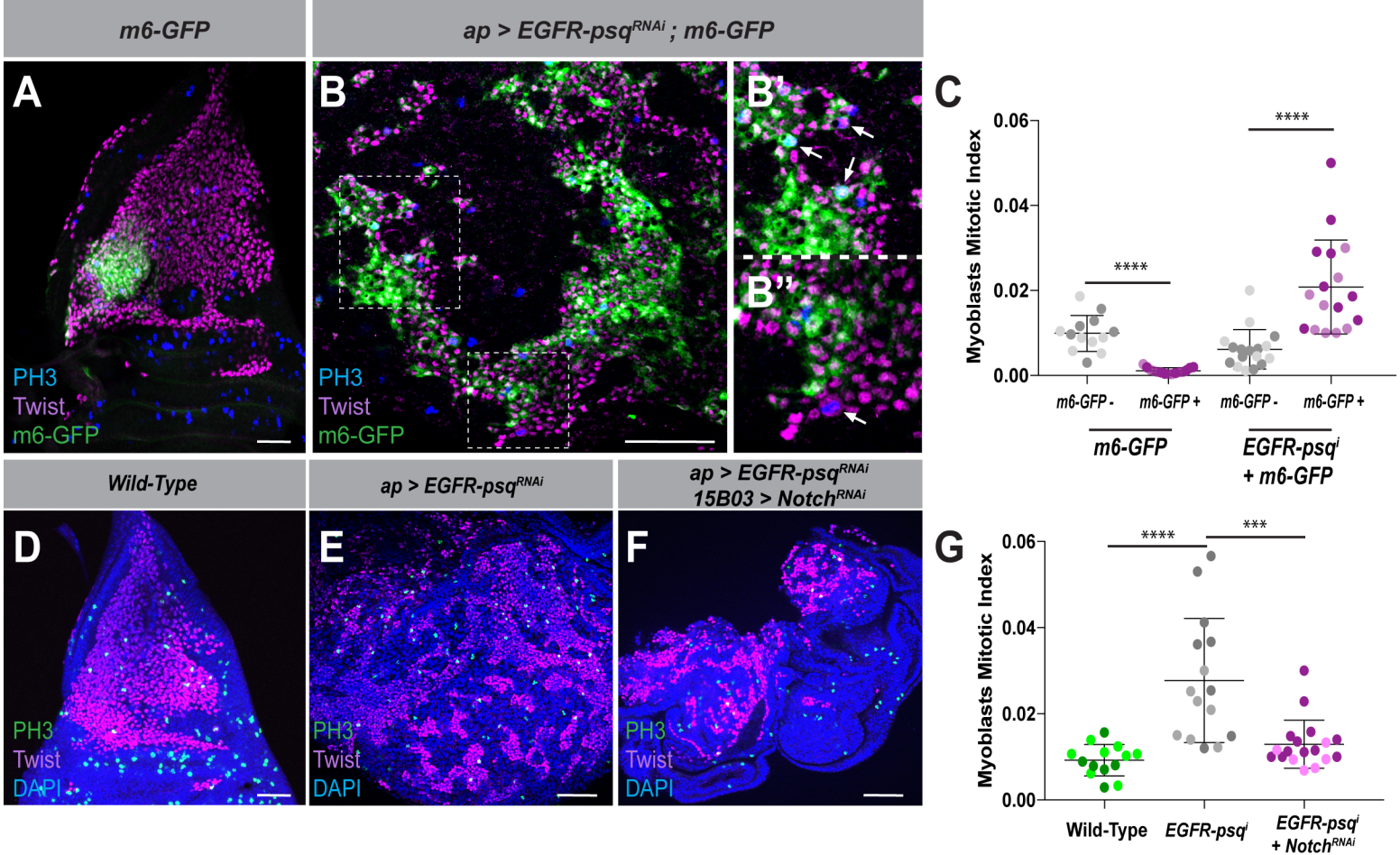
m6-GFP
ap > EGFR-psq^RNAi ; m6-GFP
A
B
B'
B''
PH3
Twist
m6-GFP
C
Myoblasts Mitotic Index
0.06
0.04
0.02
0.00
****
****
m6-GFP -
m6-GFP +
m6-GFP -
m6-GFP +
m6-GFP
EGFR-psq^i
+ m6-GFP
Wild-Type
ap > EGFR-psq^RNAi
ap > EGFR-psq^RNAi
15B03 > Notch^RNAi
D
E
F
PH3
Twist
DAPI
G
Myoblasts Mitotic Index
0.06
0.04
0.02
0.00
****
***
Wild-Type
EGFR-psq^i
EGFR-psq^i
+ Notch^RNAi

Figure 5

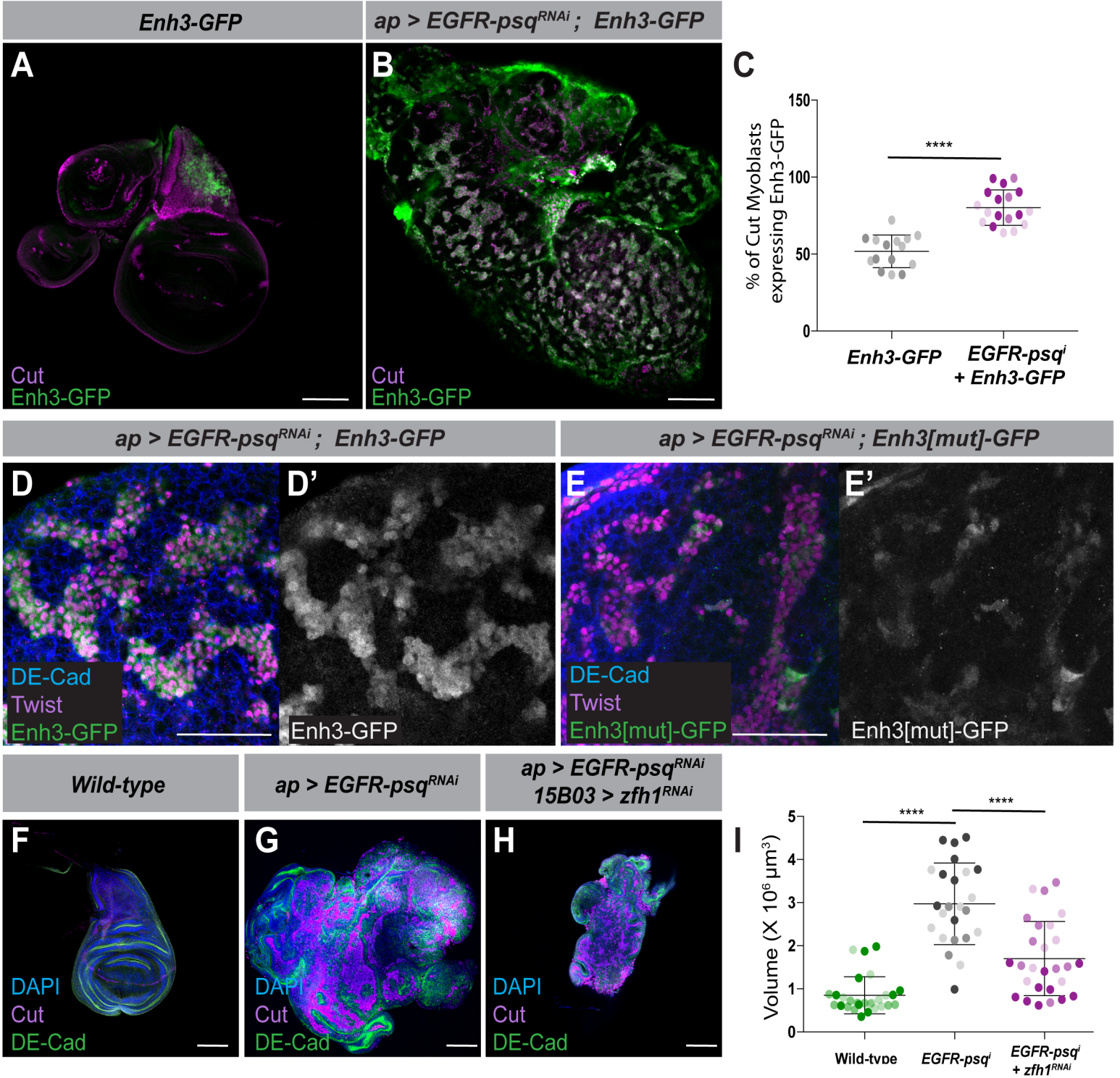
Enh3-GFP
ap > EGFR-psq^RNAi ; Enh3-GFP
A
Cut
Enh3-GFP
B
Cut
Enh3-GFP
C
% of Cut Myoblasts expressing Enh3-GFP
150
100
50
0
****
Enh3-GFP
EGFR-psq^i + Enh3-GFP
ap > EGFR-psq^RNAi ; Enh3-GFP
ap > EGFR-psq^RNAi ; Enh3[mut]-GFP
D
DE-Cad
Twist
Enh3-GFP
D'
Enh3-GFP
E
DE-Cad
Twist
Enh3[mut]-GFP
E'
Enh3[mut]-GFP
Wild-type
ap > EGFR-psq^RNAi
ap > EGFR-psq^RNAi 15B03 > zfh1^RNAi
F
DAPI
Cut
DE-Cad
G
DAPI
Cut
DE-Cad
H
DAPI
Cut
DE-Cad
I
Volume (X 10^6 µm^3)
5
4
3
2
1
0
****
****
Wild-type
EGFR-psq^i
EGFR-psq^i + zfh1^RNAi

Figure 6

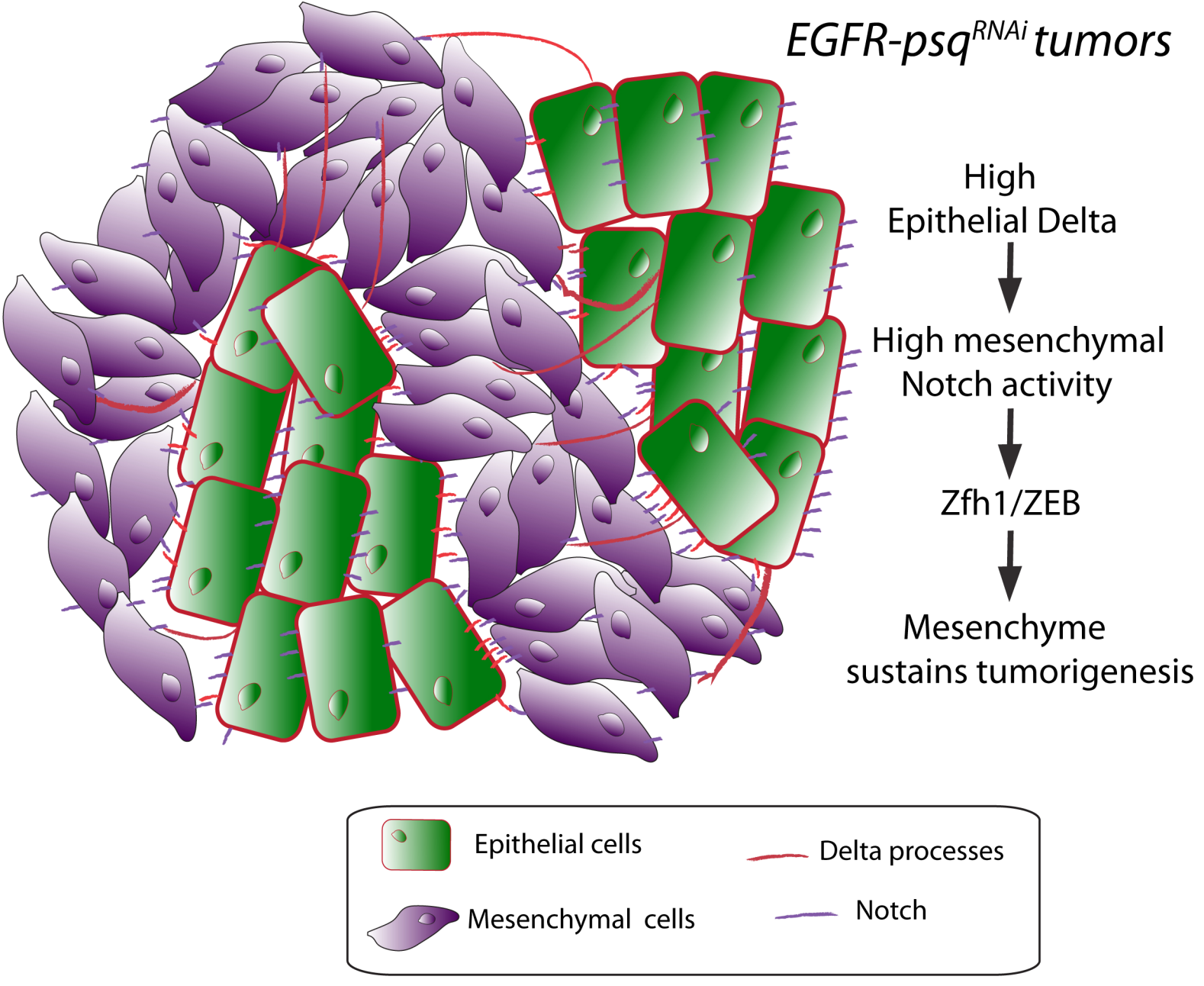
EGFR-psq^RNAi tumors
High
Epithelial Delta
High mesenchymal
Notch activity
Zfh1/ZEB
Mesenchyme
sustains tumorigenesis
Epithelial cells
Mesenchymal cells
Delta processes
Notch

Figure 7

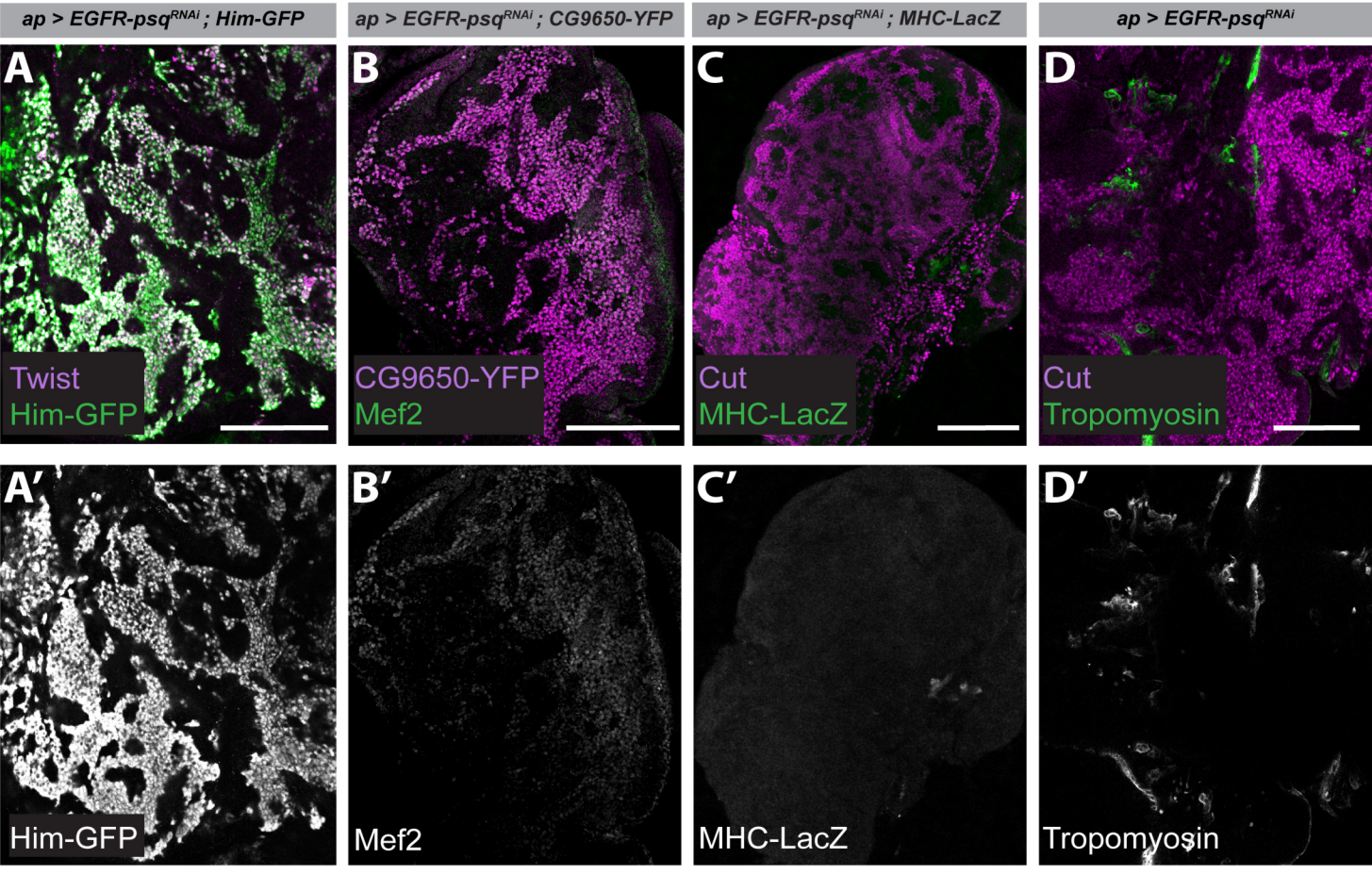
ap > EGFR-psq^RNAi ; Him-GFP
ap > EGFR-psq^RNAi ; CG9650-YFP
ap > EGFR-psq^RNAi ; MHC-LacZ
ap > EGFR-psq^RNAi
A
Twist
Him-GFP
B
CG9650-YFP
Mef2
C
Cut
MHC-LacZ
D
Cut
Tropomyosin
A'
Him-GFP
B'
Mef2
C'
MHC-LacZ
D'
Tropomyosin

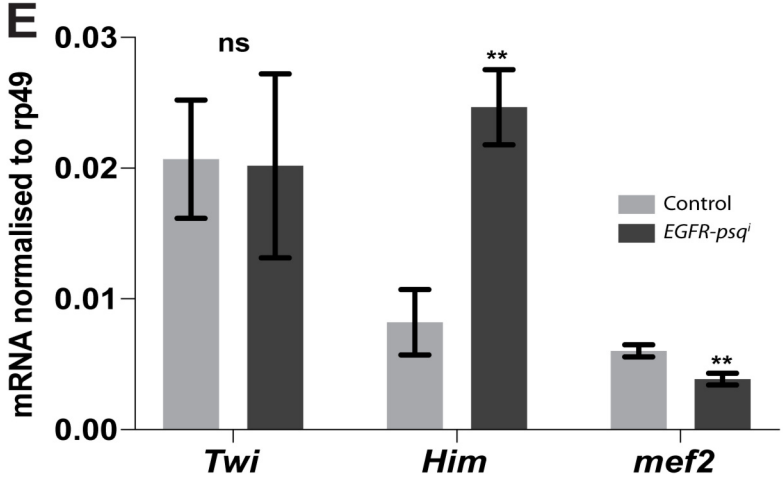
E
mRNA normalised to rp49
0.03
0.02
0.01
0.00
ns
**
**
Control
EGFR-psq^i
Twi
Him
mef2

Figure S1. Tumor mesenchymal cells are maintained undifferentiated. Related to Figure 1.

(A-D') *ap* > *EGFR-psq*^{RNAi} wing discs dissected 8-10 days after Gal4 induction stained for the following progenitor and differentiation markers. (**A-A'**) Him-GFP (Green) and Twist (Magenta). (**B-B'**) CG9650-YFP (Magenta) and Mef2 (Green). (**C-C'**) MHC-LacZ (Green) and Cut (Magenta). (**D-D'**) Tropomyosin (Green) and Cut (Magenta). The genotypes are indicated above each panel. Scale bars: 100μm. (**E**) *Twist*, *Him* and *Mef2* mRNA expression levels measured by quantitative RT-PCR. RNAs were prepared from three independent experiments. Error bars represent s.e.m.

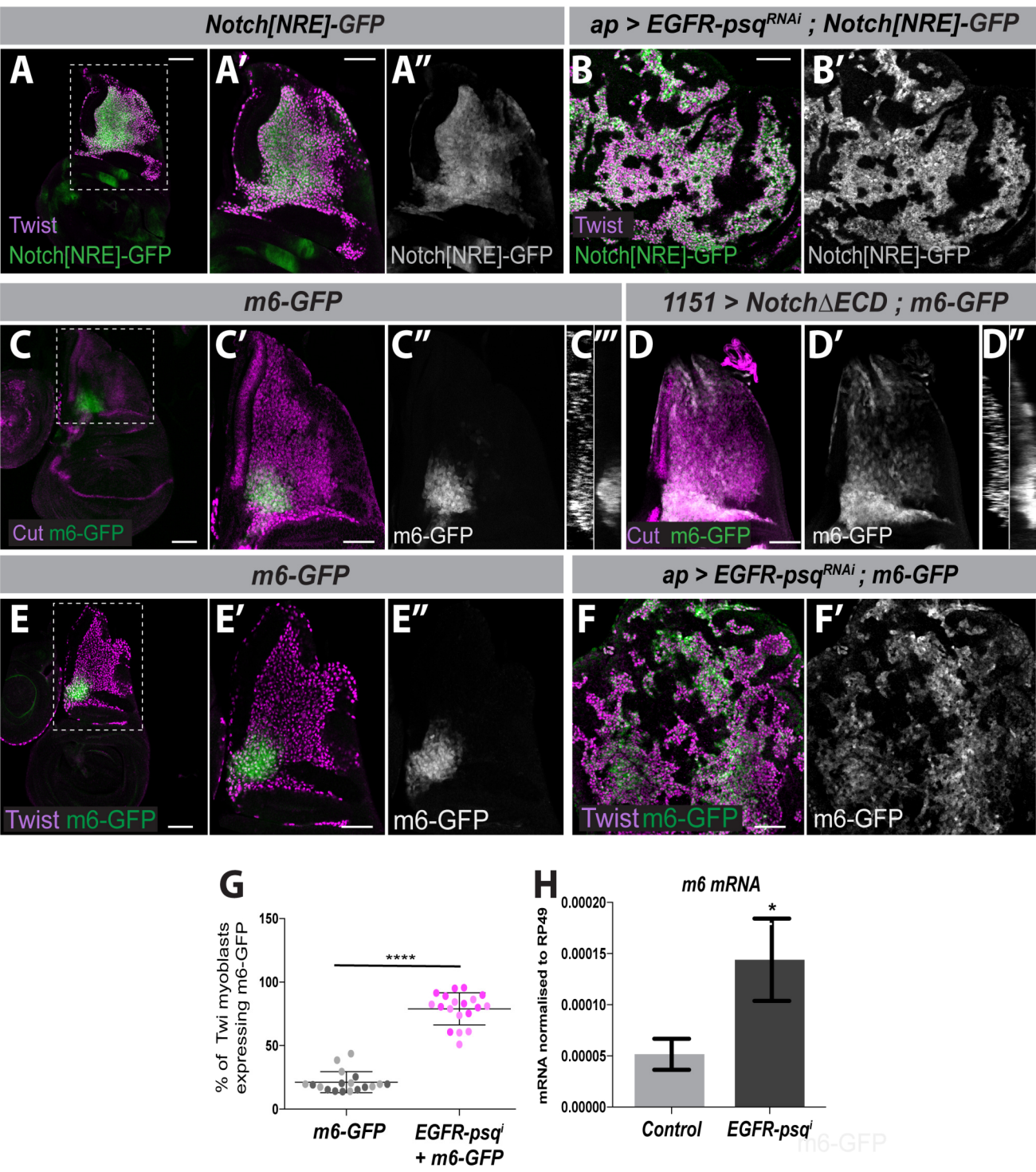
Notch[NRE]-GFP
ap > EGFR-psq^RNAi ; Notch[NRE]-GFP
A
A'
A''
B
B'
Twist
Notch[NRE]-GFP
Notch[NRE]-GFP
Twist
Notch[NRE]-GFP
Notch[NRE]-GFP
m6-GFP
1151 > NotchΔECD ; m6-GFP
C
C'
C''
C'''
D
D'
D''
Cut m6-GFP
m6-GFP
Cut m6-GFP
m6-GFP
m6-GFP
ap > EGFR-psq^RNAi ; m6-GFP
E
E'
E''
F
F'
Twist m6-GFP
m6-GFP
Twist m6-GFP
m6-GFP
G
% of Twi myoblasts expressing m6-GFP
150
100
50
0
****
m6-GFP
EGFR-psq^i + m6-GFP
H
m6 mRNA
mRNA normalised to RP49
0.00020
0.00015
0.00010
0.00005
0.00000
*
Control
EGFR-psq^i

Figure S2. Notch activity is up regulated in the mesenchymal cells during tumor growth. Related to Figure 1.

(**A-B'**) Expression of *Notch[NRE]-GFP* reporter (Green) and myoblast marker Twist (Magenta) in wild type myoblasts (**A-A'')** and in mesenchyme of *ap> EGFR-psq*^{RNAi} tumors (**B-B')**. **(A'-A'')** Higher magnifications of the boxed region in **A**. **(C-D')** Expression of an activated Notch (D-D"; 1151-Gal4>UAS-NΔECD) induces ectopic *m6-GFP* (GFP, Green) in the myoblasts (Cut, Magenta) in comparison with wild type (C-C'''). **(E-F)** Expression of *m6-GFP* reporter (green) is detected in a small group of myoblasts (Twist, Magenta) in wild type (**E-E''**) but is widely upregulated throughout the mesenchyme (Twist, Magenta) in *ap>EGFR-psq*^{RNAi} tumors (**F-F'**). (**G**) Proportions of myoblasts expressing *m6-GFP* in the indicated genotypes (****p<0.0001, Mann–Whitney *U* test, n=18 wild type, n=19 tumorous wing discs, light and dark shading indicates data points from two independent replicates). **(H)** *m6* mRNA expression level measured by quantitative RT-PCR. RNAs were prepared from wild type wing discs or *ap>EGFR-psq*^{RNAi} tumors obtained from three independent experiments. *p<0.05, unpaired Student's t-test comparing wild type and tumorous wing discs. Error bars represent s.e.m.

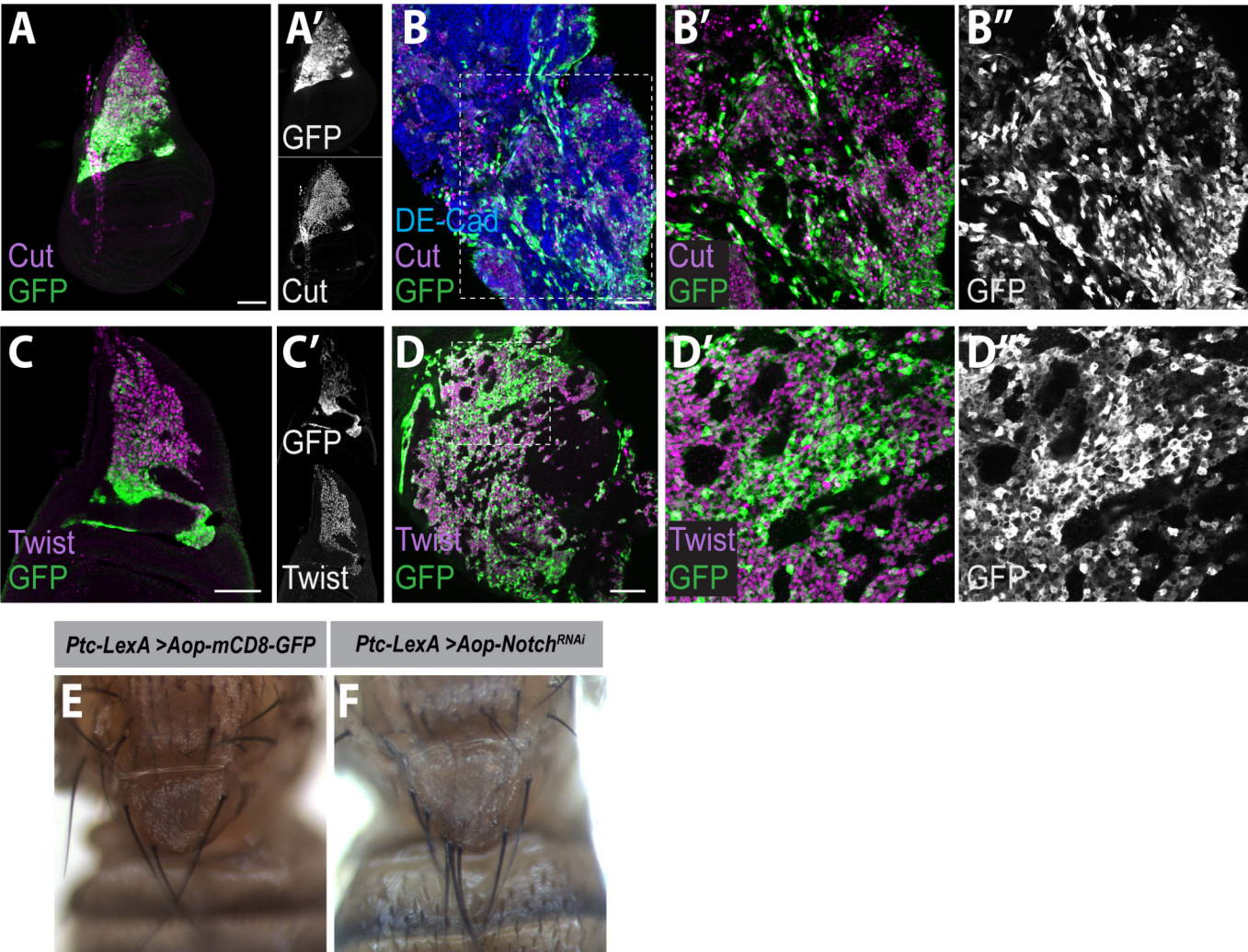
15B03-LexA > Aop-mCD8-GFP
ap > EGFR-psq^RNAi
15B03-LexA > Aop-mCD8-GFP
A
Cut
GFP
A′
GFP
Cut
B
DE-Cad
Cut
GFP
B′
Cut
GFP
B″
GFP
C
Twist
GFP
C′
GFP
Twist
D
Twist
GFP
D′
Twist
GFP
D″
GFP
Ptc-LexA >Aop-mCD8-GFP
Ptc-LexA >Aop-Notch^RNAi
E
F

Figure S3. *15B03-lexA* driver is expressed in wild type and tumorous wing disc myoblasts. Related to Figure 1.

(**A-D''**) Expression of *15B03-LexA* driver (detetced with GFP, Green) in wild type (**A,C**) and tumorous (**B,D**) wing discs. Myoblasts (Magenta) are marked with Cut (**A-B''**) or Twist (**C-D''**). B' and D' are higher magnifications of boxed regions in B and D, respectivelly. Scale bars: 50μm. (**E-F**) Increased numbers of scutellar bristles were observed when expression of *LexAop-Notch*^{RNAi} was driven with *patched-LexA*.

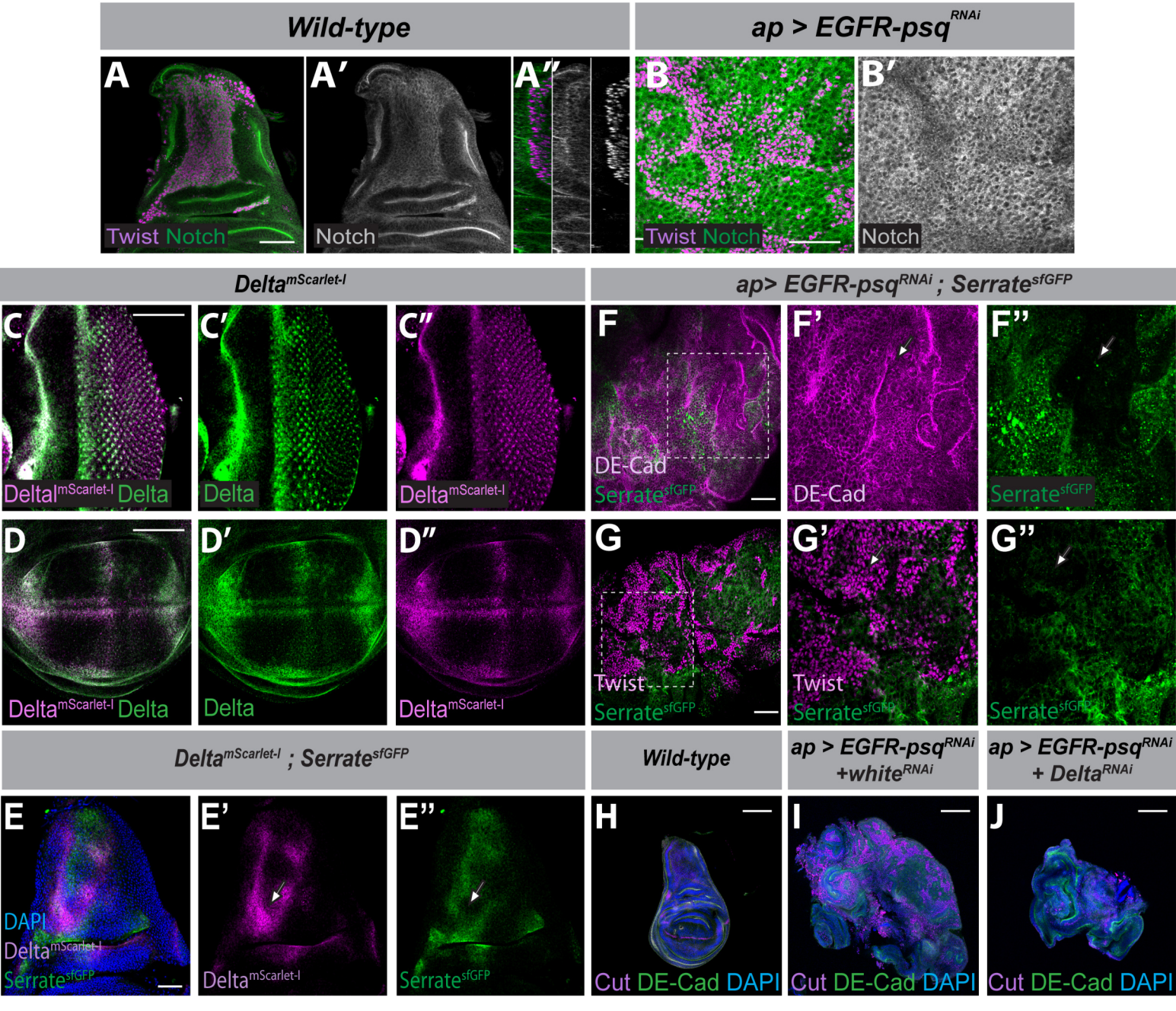
Wild-type
ap > EGFR-psq RNAi
A
A'
A''
B
B'
Twist Notch
Notch
Twist Notch
Notch
Delta mScarlet-I
ap> EGFR-psq RNAi ; Serrate sfGFP
C
C'
C''
F
F'
F''
Delta mScarlet-I Delta
Delta
Delta mScarlet-I
DE-Cad
Serrate sfGFP
DE-Cad
Serrate sfGFP
D
D'
D''
G
G'
G''
Delta mScarlet-I Delta
Delta
Delta mScarlet-I
Twist
Serrate sfGFP
Twist
Serrate sfGFP
Serrate sfGFP
Delta mScarlet-I ; Serrate sfGFP
Wild-type
ap > EGFR-psq RNAi +white RNAi
ap > EGFR-psq RNAi + Delta RNAi
E
E'
E''
H
I
J
DAPI
Delta mScarlet-I
Serrate sfGFP
Delta mScarlet-I
Serrate sfGFP
Cut DE-Cad DAPI
Cut DE-Cad DAPI
Cut DE-Cad DAPI

Figure S4. Expression of Notch, Delta$^{mScarlet-I}$ and Serrate^{sfGFP} in wild type and tumorous discs. Related to Figures 2.

(A-B') Distribution of Notch (anti-NICD, Green) in wild type wing discs (A-A'') and *ap> EGFR-psq^{RNAi}* tumors (B-B'). Twist marks myblasts (Magenta). **(A''')** Optical cross-sections of wild type. **(C-D'')** Comparison of Delta (Green) and Delta$^{mScarlet-I}$ (Magenta) expression in eye (**C-C''**) and wing discs (**D-D''**); Delta$^{mScarlet-I}$ reliably reproduces the expression pattern of Delta. (**E-E''**) Comparison of Delta (Delta$^{mScarlet-I,}$ Magenta) and Serrate (Serrate^{sfGFP}, Green) expression in wing disc epithelial cells (notum); low levels of Serrate are detected in the region with high levels of Delta (arrows in **E'**, **E''**). Scale bars: 50µm. (**F-F''**) Serrate^{sfGFP} (Green) exhibits variable expression in *ap>EGFR-psq^{RNAi}* epithelial cells (DE-Cad, Magenta; arrows in **F', F''**). **F'-F''** are individual channels of framed region in **F**. (**G-G''**) Serrate^{sfGFP} (Green) is not detected the mesenchymal cells (Twist, Magenta). **G'** and **G''** are individual channels of framed region in **G**. Genotypes are indicated in the figure. **(H-J)** Epithelial Delta expression is required for tumor-growth. Wild-type (**H**), *ap>EGFR-psq^{RNAi}; UAS-white^{RNAi}* (**I**) and *ap> EGFR-psq^{RNAi}; UAS-Delta^{RNAi}* (**J**) discs stained with anti-Cut (Magenta), anti-DE-Cad (Green) and DAPI (Blue). Scale bars: 100µm.

ap > EGFR-psq^{RNAi} + CD8-GFP; Dl$^{mScarlet-I}$

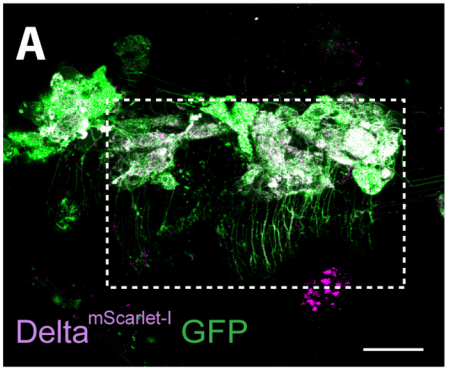

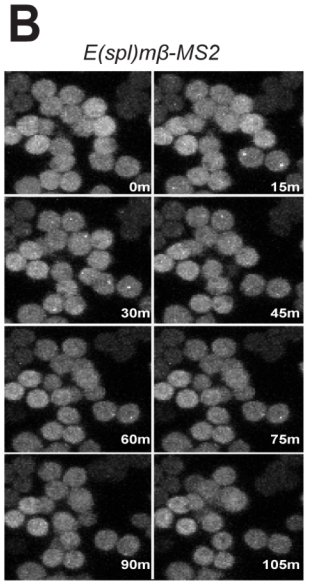

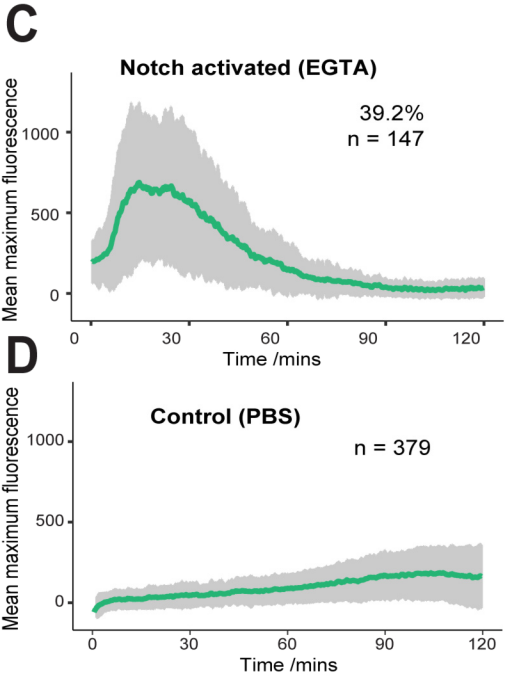

Figure S5. *E(spl)mβ-HLH* transcription is detected within short timeframe after Notch activation. Related to Figures 3 and 4.

(A) Lower magnification image of the sample shown in Figure 3A-B', a maximum Z-stack projection illustrates both apical and basal views**.** Scale bar: 20μm. **(B)** *mβ*-MS2 cells at the time points indicated after Notch activation by EGTA treatment. Transcriptional foci are detected 10-15 minutes after Notch activation. (**C**) Mean of maximum *E(spl)mβ-HLH* transcriptional fluorescence from responding cells, error-bars indicate s.e.m. *E(spl)mβ-HLH* transcription is upregulated and subsequently down-regulated over a period of approximately 60 minutes. (**D**) Transcriptional spots are not detected under control conditions (treatment with PBS only).

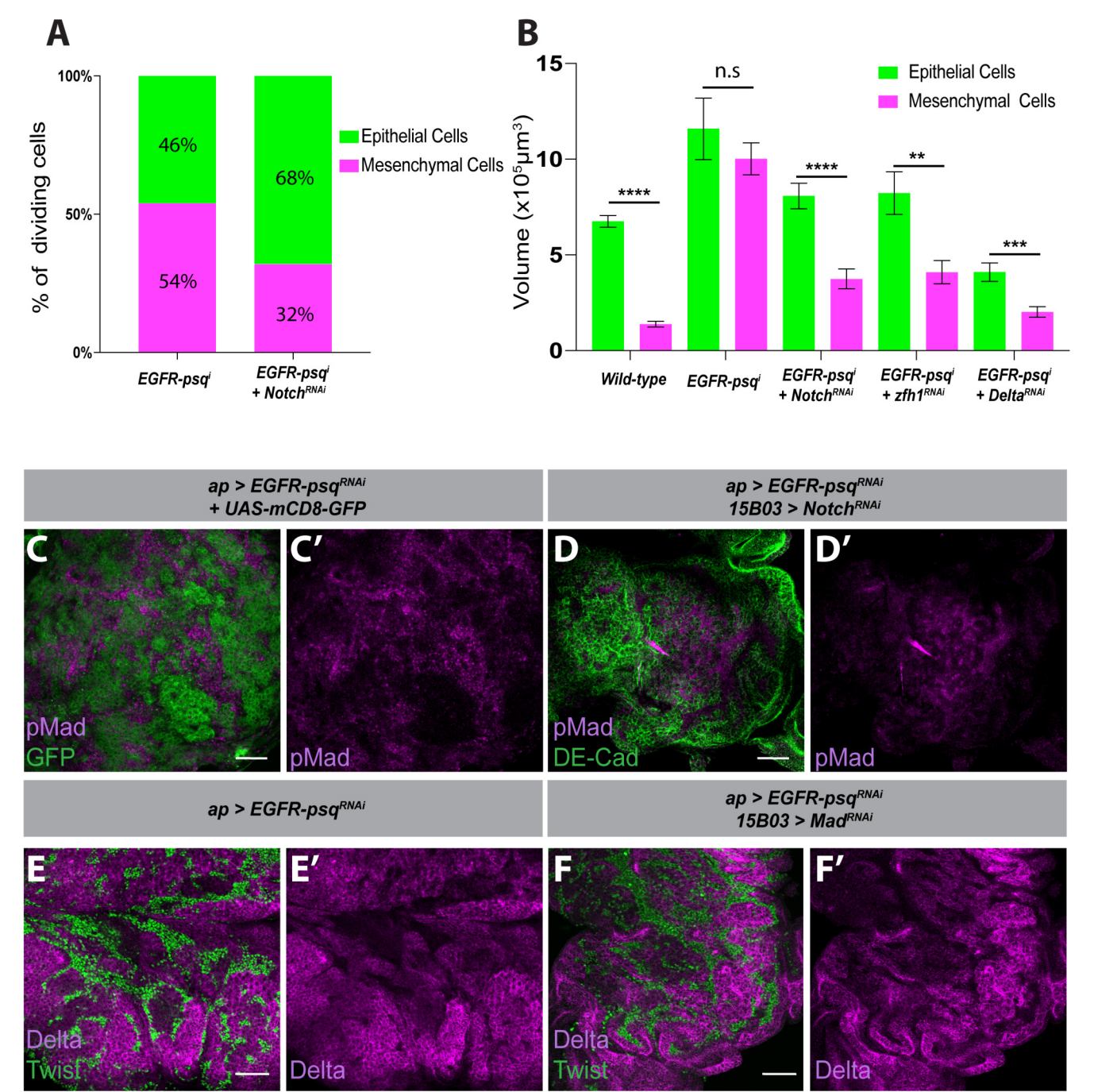
A
100%
50%
0%
% of dividing cells
46%
54%
68%
32%
Epithelial Cells
Mesenchymal Cells
EGFR-psq^i
EGFR-psq^i + Notch^RNAi
B
15
10
5
0
Volume (x10^5µm^3)
n.s
****
****
**
***
Epithelial Cells
Mesenchymal Cells
Wild-type
EGFR-psq^i
EGFR-psq^i + Notch^RNAi
EGFR-psq^i + zfh1^RNAi
EGFR-psq^i + Delta^RNAi
ap > EGFR-psq^RNAi + UAS-mCD8-GFP
ap > EGFR-psq^RNAi 15B03 > Notch^RNAi
C
pMad
GFP
C'
pMad
D
pMad
DE-Cad
D'
pMad
ap > EGFR-psq^RNAi
ap > EGFR-psq^RNAi 15B03 > Mad^RNAi
E
Delta
Twist
E'
Delta
F
Delta
Twist
F'
Delta

Figure S6. Notch and Dpp pathways operate in parallel to promote tumor growth. Related to Figure 5.

(A) Proportion of dividing mesenchymal (Magenta) and epithelial cells (Green) in *ap>EGFR-psq*^{RNAi} tumors (n=24 samples from two replicates) and *ap>EGFR-psq*^{RNAi} tumors where mesenchymal *Notch* is depleted (*15B03-lexA; LexAop-Notch*^{RNAi}; n=30 samples from two replicates). **(B)** Comparison of epithelial and mesenchymal volumes in the indicated genotypes. Wild type, ****p<0.0001; *>Notch*^{RNAi}, ****p<0.0001; *>Delta*^{RNAi}, ***p=0.0002; *>Zfh1*^{RNAi}, **p=0.01 (unpaired t-test)**. (C-D)** Depleting *Notch* in the mesenchymal cells does not affect p-Mad expression (Magenta). (**E-F'**). Depleting *Mad* in the mesenchymal cells (Twist, Green) does not affect levels of Delta (Magenta) in the epithelium. Genotypes are indicated in the figure. Scale bars: 50μm.

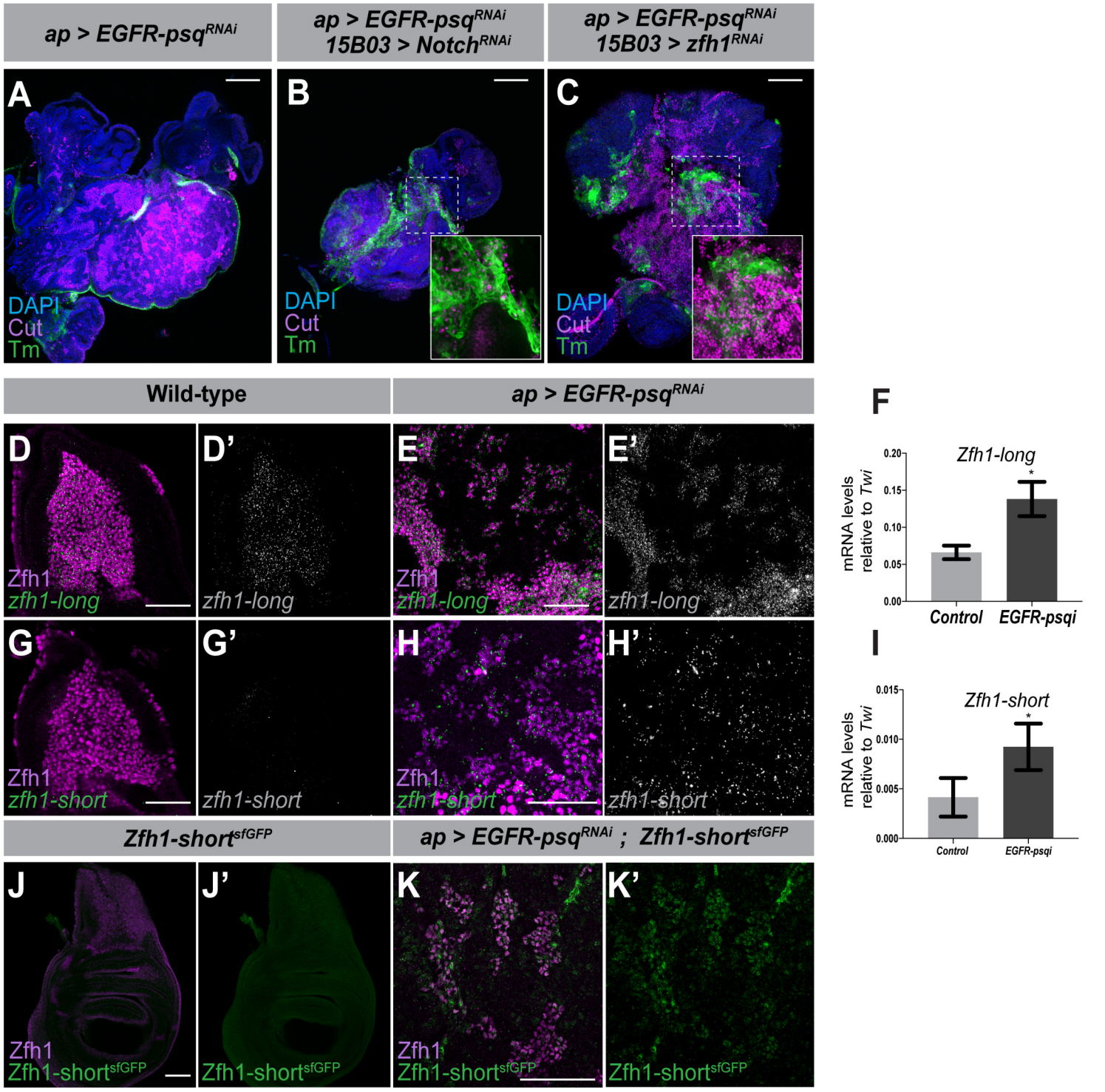
ap > EGFR-psq^RNAi
ap > EGFR-psq^RNAi 15B03 > Notch^RNAi
ap > EGFR-psq^RNAi 15B03 > zfh1^RNAi
A
B
C
DAPI
Cut
Tm
Wild-type
ap > EGFR-psq^RNAi
D
D'
E
E'
Zfh1
zfh1-long
G
G'
H
H'
zfh1-short
F
Zfh1-long
mRNA levels relative to Twi
0.20
0.15
0.10
0.05
0.00
Control
EGFR-psqi
I
Zfh1-short
0.015
0.010
0.005
0.000
Zfh1-short^sfGFP
ap > EGFR-psq^RNAi ; Zfh1-short^sfGFP
J
J'
K
K'

Figure S7. Notch and *zfh1* are required to prevent differentiation of mesenchymal cells in *ap>EGFR-psq^{RNAi}* tumors. Related to Figure 6.

(**A**) In unmanipulated *ap>EGFR-psq^{RNAi}* tumors, mesenchymal cells (Cut, Magenta) do not express Tropomyosin (Green). *ap>EGFR-psq^{RNAi}* tumors where *Notch* (**B**) or *zfh1* (**C**) were down-regulated in mesenchyme exhibit Tropomyosin expression, indicative of premature differentiation. Scale bars: 100μm. (**B' and C'**) Higher magnification of boxed regions in (**B,C**). Scale bars: 50μm. (**D-K'**) *zfh1/ZEB* expression is up-regulated in *ap> EGFR-psq^{RNAi}* tumors. Expression of *zfh1-long* **(D-E')** and *zfh1-short* (**G-H'**) isoforms in wild type and *ap> EGFR-psq^{RNAi} tumor* mesenchymal cells. Scale bars: 50μm. *zfh1-long* (**F**) and *zfh1-short* (**I**) mRNA expression level measured by quantitative RT-PCR from wild type or *ap>EGFR-psq^{RNAi}* tumors wing discs (n=3 independent experiments; * $p<0.05$, unpaired Student's t-test. Error bars represent s.e.m. (**J-K**) Zfh1-short^{sfGFP} (Green) expression is undetected in wildtype (**J**) but is present in mesenchyme of *ap>EGFR-psq^{RNAi}* tumors (**K**). Zfh1, Magenta, marks mesenchyme; scale bars: 50μm.

Genotypes	Additional information
ap > mCD8-GFP	*y w; Ap-Gal4 / UAS-mCD8-GFP*
ap > EGFR-psq^{RNAi}	*y w; Ap-Gal4, UAS-psq^{RNAi}; UAS-EGFR, tub-Gal80ts*
ap > EGFR-psq^{RNAi} + mCD8-GFP	*y w; Ap-Gal4, UAS-psq^{RNAi} / UAS-mCD8-GFP; UAS-EGFR, tub-Gal80ts/+*
ap > EGFR-psq^{RNAi} ; Notch[NRE]-GFP	*y w; Ap-Gal4, UAS-psq^{RNAi} / Notch[NRE]-GFP; UAS-EGFR, tub-Gal80ts/+*
ap > EGFR-psq^{RNAi}; m6-GFP	*y w; Ap-Gal4, UAS-psq^{RNAi} / m6-GFP; UAS-EGFR, tub-Gal80ts/+*
ap > EGFR-psq^{RNAi} 15B03 > Notch^{RNAi}	*y w; Ap-Gal4, UAS-psq^{RNAi} / 15B03-LexA; UAS-EGFR, tub-Gal80ts / Lex-Aop-Notch^{RNAi}*
ap > EGFR-psq^{RNAi}; Dl$^{mScarlet-I}$	*y w; Ap-Gal4, UAS-psq^{RNAi} / + ; UAS-EGFR, tub-Gal80ts/ Delta$^{mScarlet-I}$*
ap > EGFR-psq^{RNAi} ; Enh3-GFP	*y w; Ap-Gal4, UAS-psq^{RNAi} /+; UAS-EGFR, tub-Gal80ts/ Enh3-GFP*
ap > EGFR-psq^{RNAi} 15B03 > Zfh1^{RNAi}	*y w; Ap-Gal4, UAS-psq^{RNAi} / 15B03-LexA; UAS-EGFR, tub-Gal80ts / Lex-Aop-Zfh1^{RNAi}*
ap > EGFR-psq^{RNAi}; Him-GFP	*y w; Ap-Gal4, UAS-psq^{RNAi} / Him-GFP; UAS-EGFR, tub-Gal80ts/+*
ap > EGFR-psq^{RNAi}; CG9650-YFP	*CG9650-YFP/+; Ap-Gal4, UAS-psq^{RNAi} /+ ; UAS-EGFR, tub-Gal80ts/+*
ap > EGFR-psq^{RNAi}; MHC-LacZ	*y w; Ap-Gal4, UAS-psq^{RNAi} / MHC-LacZ; UAS-EGFR, tub-Gal80ts/+*
1151 > NotchΔECD; m6-GFP	*1151-Gal4; UAS-NotchΔECD/m6-GFP*
ap > EGFR-psq^{RNAi} 15B03-LexA > Aop-mCD8-GFP	*y w; Ap-Gal4, UAS-psq^{RNAi} / 15B03-LexA; UAS-EGFR, tub-Gal80ts / Lex-Aop-mCD8-GFP*
ap > EGFR-psq^{RNAi} + white^{RNAi}	*y w; Ap-Gal4, UAS-psqRNAi /+ ; UAS-EGFR, tub-Gal80ts/UAS-whiteRNAi*
ap > EGFR-psq^{RNAi} + Delta^{RNAi}	*y w; Ap-Gal4, UAS-psq^{RNAi} /+ ; UAS-EGFR, tub-Gal80ts/UAS-Delta^{RNAi}*
ap > EGFR-psq^{RNAi}; Serrate^{sfGFP}	*y w; Ap-Gal4, UAS-psq^{RNAi} /+ ; UAS-EGFR, tub-Gal80ts/Serrate^{sfGFP}*
ap > EGFR-psq^{RNAi}; m6-GFP + Dia^{RNAi}	*y w; Ap-Gal4, UAS-psq^{RNAi} /m6-GFP ; UAS-EGFR, tub-Gal80ts/UAS-Dia^{RNAi}*

Table S1. Full genotypes of samples analyzed. Related to Figures 1 to 6 and S1 to S7.

Name	Sequence
Notch forward	GGTCATCATTGCATTGGCC
Notch reverse	CTCATCCTTATCGTCCTGGG
zfh1 forward	CCAGTGCATAGAGTGTCCGA
zfh1 reverse	ACCTGAACTCGACGACGG
E(spl)-mβ-HLH	GTCGGGACGCCACATGGGGCCAG
Rpl32 forward	ATGCTAAGCTGTCGCACAAATG
Rpl32 reverse	GTTCGATCCGTAACCGATGT
Mef2 forward	TCCTGCTCAAGTACACCGAG
Mef2 reverse	CGCTGCATCATGTTCTGGAA
Twist forward	CCTCTACAACAACCAGCAGC
Twist reverse	ACTCCATGTCATCCCGATCC
Him forward	CAATGCAATCTGGCCATCGA
Him reverse	TCGAAGATCTGGTGGCGAAT
E(spl)-m6 forward	GTAAAGAACTTATTGGCCAAAATG
E(spl)-m6 reverse	CTGCGAGTGCCAGTAGAAGC
zfh1-long forward	GACGAGCAGAGCAACATGAG
zfh1-long reverse	CGCTGTTGTTGTTCATGGACTG
zfh1-short forward	AGAAACACACACGCAGCAAA
zfh1-short reverse	TTGGGGTCGTGTTTAGGGAA

Table S2. List of oligonucleotides. Related to STAR methods.